

Provably Efficient Online RLHF with One-Pass Reward Modeling

Long-Fei Li*, Yu-Yang Qian*, Peng Zhao, Zhi-Hua Zhou

National Key Laboratory for Novel Software Technology, Nanjing University, China
 School of Artificial Intelligence, Nanjing University, China,
 {lilf, qianyy, zhaop, zhoush}@lamda.nju.edu.cn

Abstract

Reinforcement Learning from Human Feedback (RLHF) has shown remarkable success in aligning Large Language Models (LLMs) with human preferences. Traditional RLHF approaches rely on a fixed dataset, which often suffers from limited coverage. To this end, online RLHF has emerged as a promising direction, enabling iterative data collection and model improvement. Despite its potential, this paradigm faces a key bottleneck: the requirement to continuously integrate new data into the historical dataset and re-optimize the model from scratch at each iteration, resulting in computational and storage costs that grow linearly with the number of iterations. In this work, we address this challenge by proposing a *one-pass* reward modeling method that does not require storing the historical data and can be computed in constant time. Specifically, we first formalize RLHF as a contextual preference bandit problem and design an online mirror descent algorithm with a tailored local norm to replace the standard maximum likelihood estimation for reward modeling. We then apply our method to various online RLHF settings, including passive data collection, active data collection, and deployment-time adaptation. We provide theoretical guarantees showing that our method improves both statistical and computational efficiency. Finally, we provide practical algorithms and conduct experiments using Llama-3-8B-Instruct and Qwen2.5-7B-Instruct models on the Ultrafeedback-binarized and Mixture2 datasets, validating the effectiveness of our proposed method.

1 Introduction

Reinforcement Learning from Human Feedback is a critical technique for training large language models using human preference feedback [Ouyang et al., 2022, Bai et al., 2022]. Typical RLHF methods involve collecting extensive data, each consisting of a prompt, a pair of responses, and a preference label indicating which response is preferred. Then, a reward model is trained to predict the human preference, and the LLM is fine-tuned based on the reward model by the RL algorithms.

Traditional RLHF methods primarily rely on fixed preference datasets, which typically suffer from limited coverage. As a result, the learned reward models struggle to generalize to out-of-distribution (OOD) samples, constraining the effectiveness of the aligned models. To address this, online RLHF has emerged as a promising paradigm, enabling iterative data collection and model improvement. The general process can be described as (i) collect the preference data; (ii) update the model using the collected preference data. The above two steps are repeated for several iterations to

*Equal contribution.

Table 1: Comparison between previous works and our work in terms of the statistical and computational efficiency across different online RLHF settings. The column “Context” and “Action” represent the context and action are determined by the environment (☉) or the algorithm (🔍). For the computational efficiency (time and storage), we highlight the dependence on the t at iteration t . Here, d is the feature dimension, T is the total number of iterations, κ is the non-linearity coefficient, $\Phi = \mathbb{E}_{x \sim \rho} [\phi(x, \pi^*(x))]$ is the concentrability vector, V_T and \mathcal{H}_T are two local norms satisfying $\|\Phi\|_{\mathcal{H}_T^{-1}} \leq \sqrt{\kappa} \|\Phi\|_{V_T^{-1}}$ (*: amortized complexity over T).

Setting	Context	Action	Gap/Regret	Time	Storage	Reference
Passive	☉	☉	$\tilde{\mathcal{O}}(\sqrt{d} \cdot \kappa \ \Phi\ _{V_T^{-1}})$	$\mathcal{O}(\log T)^*$	$\mathcal{O}(t)$	Zhu et al. [2023]
			$\tilde{\mathcal{O}}(\sqrt{d} \cdot \ \Phi\ _{\mathcal{H}_T^{-1}})$	$\mathcal{O}(1)$	$\mathcal{O}(1)$	Ours (Theorem 1)
Active	🔍	🔍	$\tilde{\mathcal{O}}(d\sqrt{\kappa/T})$	$\mathcal{O}(t \log t)$	$\mathcal{O}(t)$	Das et al. [2024]
			$\tilde{\mathcal{O}}(d\sqrt{\kappa/T})$	$\mathcal{O}(1)$	$\mathcal{O}(1)$	Ours (Theorem 2)
Deployment	☉	🔍	$\tilde{\mathcal{O}}(d\kappa\sqrt{T})$	$\mathcal{O}(t \log t)$	$\mathcal{O}(t)$	Saha et al. [2023]
			$\tilde{\mathcal{O}}(d\sqrt{\kappa T})$	$\mathcal{O}(1)$	$\mathcal{O}(1)$	Ours (Theorem 3)

boost model performance. In practice, the Claude [Bai et al., 2022] and LLaMA-2 [Touvron et al., 2023] projects have demonstrated that online RLHF can significantly enhance model performance.

Despite its empirical success, online RLHF introduces significant computational challenges. Specifically, the typical process of online RLHF involves continuously integrating newly collected data into the dataset and re-optimizing the model from scratch over the expanded dataset. While this strategy is statistically efficient, its computational and storage costs scale linearly with the number of iterations, which becomes prohibitive in long-term iterations, especially on edge devices where computation and memory resources are inherently limited. This raises a pressing question:

Can we design online RLHF algorithms that are both statistically and computationally efficient?

In this work, we provide an affirmative answer to this question in the setting of contextual preference bandits with linearly parameterized reward functions. Specifically, building on recent theoretical advancements in RLHF [Zhu et al., 2023, Das et al., 2024, Ji et al., 2024], we formulate the RLHF problem as a contextual dueling bandit problem [Yue et al., 2012, Saha, 2021]. While prior work has explored this formulation, most existing methods focus on statistical efficiency and overlook the growing computational burden. To bridge this gap, we introduce a novel *one-pass* reward modeling algorithm which does not require storing the historical data and can be computed in constant time. Our method is based on the online mirror descent framework with a tailored local norm that captures second-order information. We then apply our method to several online RLHF settings, including passive data collection, active data collection, and deployment-time adaptation. We establish theoretical guarantees showing that our method improves both statistical and computational efficiency. Table 1 summarizes the comparison of our method with the existing methods.

To enable usage in LLMs, we develop practical variants of our method. Direct computation and storage of the Hessian matrix is prohibitively expensive; thus, we propose an efficient approximation using Hessian-Vector Products (HVP) combined with conjugate gradient descent, avoiding explicit second-order information and relying only on first-order computation. Additionally, we employ rejection sampling to approximate model uncertainty in a computationally efficient manner. With the above techniques, we conduct experiments using the LLaMA-3-8B-Instruct [Llama Team, 2023] and Qwen2.5-7B-Instruct [Qwen Team, 2024] models on the Ultrafeedback-binarized [Cui et al., 2023] and Mixture2 [Dong et al., 2024] datasets, validating the effectiveness of our method.

To summarize, our contributions are as follows:

- By formulating the RLHF problem as a contextual dueling bandit, we propose a novel one-pass reward modeling algorithm and establish the corresponding estimation error bound. Our method is built upon the online mirror descent framework and incorporates a carefully designed local norm that captures second-order information for improved learning efficiency.
- We apply our method to a broad range of online RLHF settings, including passive data collection, active data collection, and deployment-time adaptation. For each setting, we design tailored algorithms and establish corresponding theoretical guarantees, demonstrating that our approach achieves improved statistical and computational efficiency than existing methods.
- We develop practical algorithms by approximating the update using Hessian-Vector Products combined with conjugate gradient descent, and estimating uncertainty via rejection sampling. Based on the above techniques, we conduct empirical evaluations using **LLaMA-3-8B-Instruct** and **Qwen2.5-7B-Instruct** models on Ultrafeedback-binarized and Mixture2 datasets, showing our method achieves better performance in both statistical and computational efficiency.

Organization. The rest of the paper is organized as follows: Section 3 introduces the problem setup. Section 4 presents our proposed one-pass reward modeling method. Section 5 applies our method to different online RLHF settings. Section 6 provides the practical implementations. Section 7 presents experimental results. Section 8 concludes the paper. We defer the proofs, experiment details, and more experimental results to the appendix.

2 Related Work

In this section, we review the works most closely related to ours, including offline RLHF, online RLHF, contextual dueling bandits, and active learning.

Offline RLHF. Learning from human preferences with deep learning models dates back to [Christian et al. \[2017\]](#) and has been recently popularized by the success of large language models [\[Bai et al., 2022, Touvron et al., 2023, Achiam et al., 2023\]](#). Existing results generally fall into two categories: reward-based and reward-free. Reward-based methods typically consist of two steps: reward modeling and reward maximization [\[Ouyang et al., 2022\]](#). Given preference data, the reward model is trained to predict preference labels, and the LLM is fine-tuned based on the reward model using RL algorithms such as PPO [\[Schulman et al., 2017\]](#). In contrast, reward-free methods directly optimize the LLM using human preference feedback, without relying on explicit reward modeling [\[Rafailov et al., 2023, Azar et al., 2024\]](#). Among these works, Direct Preference Optimization (DPO) [\[Rafailov et al., 2023\]](#) is one of the most popular reward-free methods, which treats generative models directly as reward models and optimizes them using human preference feedback. Given the empirical success of RLHF, recent efforts have been devoted to developing a deeper theoretical understanding of this approach. [Zhu et al. \[2023\]](#) proposed to formulate RLHF as a contextual preference bandit problem and proved the maximum likelihood estimator converges under both the Bradley-Terry (BT) model and Plackett-Luce (PL) model with linear reward functions.

Online RLHF. Offline RLHF methods rely on fixed preference datasets, which often suffer from limited data coverage. Consequently, the resulting reward models struggle to generalize to out-of-distribution samples, thereby limiting the effectiveness of the aligned models. To overcome this limitation, online RLHF has emerged as a promising alternative, enabling iterative data collection and continuous model refinement. The works [Dong et al., 2023, Guo et al., 2024, Yuan et al., 2024, Wu et al., 2025] have demonstrated that online iterative variants of direct preference learning algorithms significantly outperform their offline counterparts. Xiong et al. [2024] identified key challenges in offline RLHF and theoretically demonstrated the potential benefits of online exploration. Recent work has incorporated optimism-driven bonus terms into the DPO loss to encourage exploration in online RLHF [Xie et al., 2025, Cen et al., 2025, Zhang et al., 2025]. These studies primarily focus on the sample efficiency, but do not consider the accompanying increase in computational complexity. In this paper, we propose algorithms that achieve both statistical and computational efficiency.

Contextual Dueling Bandits and RL. Dueling bandits are a variant of the multi-armed bandit problem in which the learner sequentially selects a pair of arms and receives noisy binary feedback [Yue et al., 2012]. The contextual dueling bandit framework extends this setting by incorporating contextual information [Dudík et al., 2015, Saha, 2021, Bengs et al., 2022]. Within this framework, Saha [2021] studied the K -armed contextual dueling bandit problem, and Saha et al. [2023] further extended it to the reinforcement learning setting. Additionally, Sekhari et al. [2024] investigated the contextual dueling bandit problem under an active learning paradigm, where the learner adaptively queries for feedback, aiming to minimize both regret and the number of queries. To move beyond linear reward functions, Verma et al. [2025] introduced the neural dueling bandit problem, modeling the reward function using neural networks. These prior works commonly rely on maximum likelihood estimation to learn the reward function, leading to computational complexity that grows linearly with the number of iterations. In contrast, we propose algorithms that maintain constant per-iteration computational complexity, while preserving statistical efficiency.

Active Learning. Active learning is a paradigm that aims to reduce the labeling cost by selecting the most informative samples for annotation [Settles, 2009]. In general, existing work can be categorized into two settings: pool-based and stream-based. The pool-based setting [Seung et al., 1992, Freund et al., 1997, Huang et al., 2010] involves the learner iteratively selecting a batch of informative samples from a large unlabeled pool, querying their labels, updating the model, and repeating this process. In contrast, the stream-based setting [Cesa-Bianchi et al., 2004, 2006, Cacciarelli and Kulahci, 2024] requires the learner to sequentially observe data points and decide in real time whether to query their labels. Within the context of RLHF, Das et al. [2024] studied pool-based active learning, while Ji et al. [2024] focused on the stream-based setting. In this work, we focus on the pool-based strategy, which can be naturally extended to the stream-based scenario.

3 Problem Setup

Following recent advancements in RLHF [Zhu et al., 2023, Das et al., 2024, Xiong et al., 2024], we formulate RLHF as a contextual bandit problem. Specifically, we have a set of contexts \mathcal{X} and a set of possible actions \mathcal{A} per context. To learn with human preference feedback, the learner selects a tuple (x, a, a') to present to the human, where $x \in \mathcal{X}$ is the context, $a, a' \in \mathcal{A}$ are the actions. The human then provides a binary preference feedback $y \in \{0, 1\}$, where $y = 1$ indicates that the

human prefers action a over action a' , and $y = 0$ otherwise. We study the commonly used Bradley-Terry (BT) model in preference learning [Bradley and Terry, 1952], which assumes that the human’s preference is generated by a logistic function of the difference in the rewards of the two actions.

Definition 1 (Bradley-Terry Model). Given a context $x \in \mathcal{X}$ and two actions $a, a' \in \mathcal{A}$, the probability of the human preferring action a over action a' is given by

$$\mathbb{P}[y = 1 \mid x, a, a'] = \frac{\exp(r(x, a))}{\exp(r(x, a)) + \exp(r(x, a'))}, \quad (1)$$

where $r : \mathcal{X} \times \mathcal{A} \rightarrow \mathbb{R}$ is a latent reward function.

We consider the widely used linear reward in the literature [Zhu et al., 2023, Cen et al., 2025].

Assumption 1. It holds that $r(x, a) = \phi(x, a)^\top \theta^*$ where $\phi(x, a) : \mathcal{X} \times \mathcal{A} \rightarrow \mathbb{R}^d$ is the known and fixed feature map, and $\theta^* \in \mathbb{R}^d$ is the unknown parameter vector. Furthermore, we assume $\|\phi(x, a)\|_2 \leq L$ for all $x \in \mathcal{X}$ and $a \in \mathcal{A}$ and $\theta^* \in \Theta$ where $\Theta = \{\theta \in \mathbb{R}^d \mid \|\theta\|_2 \leq B\}$.

Remark 1. The feature mapping ϕ can be constructed by removing the last layer of a pre-trained large language model, and θ^* corresponds to the weights of the last layer.

Then, we can rewrite the probability as $\mathbb{P}[y = 1 \mid x, a, a'] = \sigma(\phi(x, a)^\top \theta^* - \phi(x, a')^\top \theta^*)$, where $\sigma(w) = \frac{1}{1 + \exp(-w)}$. Next, we introduce a key quantity that captures learning complexity.

Definition 2. The non-linearity coefficient κ is defined as

$$\kappa = \max_{x \in \mathcal{X}, a, a' \in \mathcal{A}} \max_{\theta \in \Theta} \frac{1}{\dot{\sigma}(\phi(x, a)^\top \theta - \phi(x, a')^\top \theta)}, \quad (2)$$

where $\dot{\sigma}(w) = \sigma(w)(1 - \sigma(w))$ is the derivative function.

The quantity κ captures the learning complexity that satisfies $\kappa \leq 2 + \exp(2BL) + \exp(-2BL)$. It may be exceedingly large with exponential dependence on the scale of features and parameters.

4 Our Framework

In this section, we first introduce the general framework for online RLHF. We then present our one-pass reward modeling method. Finally, we show the theoretical guarantee of our method.

4.1 General Framework for Online RLHF

The general process of online RLHF involves iteratively collecting data and updating the model based on the collected data. At iteration t , the process can be formulated as:

- (i) **New data collection:** Sample a prompt x_t and two responses a_t and a'_t , query the oracle to obtain the preference label $y_t \in \{0, 1\}$, expand the dataset $\mathcal{D}_{t+1} = \mathcal{D}_t \cup \{(x_t, a_t, a'_t, y_t)\}$.
- (ii) **Reward modeling:** Train a reward model r_{t+1} using the historical dataset \mathcal{D}_{t+1} .
- (iii) **Policy optimization (Optional):** Update the policy π_{t+1} using the reward model r_{t+1} .

A key challenge in online RLHF is that the reward model needs to be trained on the entire historical dataset at each iteration, which is computationally expensive. Specifically, let $z_t = \phi(x_t, a_t) - \phi(x_t, a'_t)$ be the feature difference, given the historical dataset $\mathcal{D}_{t+1} = \{(x_i, a_i, a'_i, y_i)\}_{i=1}^t$, the reward model is estimated via maximum likelihood estimation as

$$\hat{\theta}_{t+1} = \arg \min_{\theta \in \mathbb{R}^d} \sum_{i=1}^t \ell_i(\theta), \text{ where } \ell_t(\theta) = -y_t \log(\sigma(z_t^\top \theta)) - (1 - y_t) \log(1 - \sigma(z_t^\top \theta)). \quad (3)$$

However, Eq. (3) does not admit a closed-form solution, requiring iterative optimization techniques, such as gradient descent, to achieve an ε -accurate estimate. As discussed by Fauray et al. [2022], obtaining such accuracy with MLE typically requires $\mathcal{O}(\log(1/\varepsilon))$ optimization steps. Since the loss function is defined over the entire historical dataset, each iteration incurs a computational cost of $\mathcal{O}(t)$ gradient evaluations. In practice, ε is often set to $1/t$ to ensure that the optimization error does not dominate the overall estimation error. As a result, the total computational complexity at iteration t becomes $\mathcal{O}(t \log t)$, a cost that is prohibitive for long-term online RLHF applications.

4.2 One-pass Reward Modeling

Drawing inspiration from recent advancements in logistic bandits [Fauray et al., 2022, Zhang and Sugiyama, 2023] and multinomial logit MDPs [Li et al., 2024], we propose a novel one-pass reward modeling method that reduces the complexity to constant time per iteration. First, define the gradient $g_t(\theta)$ and Hessian $H_t(\theta)$ of loss $\ell_t(\theta)$ as $g_t(\theta) = (\sigma(z_t^\top \theta) - y_t)z_t$ and $H_t(\theta) = \dot{\sigma}(z_t^\top \theta)z_t z_t^\top$.

Implicit OMD. To improve the computational efficiency, Fauray et al. [2022] observed that the cumulative past log-loss is strongly convex and can therefore be well approximated by a quadratic function. Building on this observation, they proposed the following update rule:

$$\bar{\theta}_{t+1} = \arg \min_{\theta \in \Theta} \left\{ \ell_t(\theta) + \frac{1}{2\eta} \|\theta - \bar{\theta}_t\|_{\bar{\mathcal{H}}_t}^2 \right\}, \quad (4)$$

where $\bar{\mathcal{H}}_t = \sum_{i=1}^{t-1} H_i(\bar{\theta}_{i+1}) + \lambda I$ is the local norm, and η is the step size. The optimization problem can be decomposed into two terms. The first term is the instantaneous log-loss $\ell_t(\theta)$, which accounts for the information of the current sample. The second consists of a quadratic proxy for the past losses constructed through the sequence $\{\bar{\theta}_i\}_{i \leq t}$. A key component is the design of the local norm $\bar{\mathcal{H}}_t$, which approximates the Hessian matrix by $H_i(\bar{\theta}_{i+1})$ at a *lookahead* point $\bar{\theta}_{i+1}$. Such a Hessian matrix effectively captures local information and is crucial for ensuring statistical efficiency.

The update rule in Eq. (4) benefits from a one-pass data processing property, which eliminates the need to store the entire historical dataset. However, the optimization problem in Eq. (4) still does not have a closed-form solution. But since the loss is defined only on the current sample, it requires only $\mathcal{O}(1)$ gradient computations per step, leading to a total computational complexity of $\mathcal{O}(\log t)$ at iteration t . This represents a significant improvement over the $\mathcal{O}(t \log t)$ complexity of the MLE estimator in Eq. (3). Nevertheless, the computational complexity of the implicit OMD is still increasing with the number of iterations, which motivates us to design a constant-time method.

Standard OMD. To enhance computational efficiency, a natural alternative is to replace this formulation with the standard OMD framework, which permits a closed-form solution and thus eliminates the need for iterative optimization. However, the standard OMD minimizes a first-order approximation of the loss function, which sacrifices several key properties compared to its implicit counterpart, as demonstrated by Campolongo and Orabona [2020]. Specifically, the

Algorithm 1 One-Pass Reward Modeling

Input: Preference data (x_t, a_t, a'_t, y_t)

- 1: Define the loss function $\ell_t(\theta)$ as Eq. (3)
- 2: Update $\tilde{\mathcal{H}}_t = \mathcal{H}_t + \eta H_t(\tilde{\theta}_t)$
- 3: Compute $\tilde{\theta}'_{t+1} = \tilde{\theta}_t - \eta \tilde{\mathcal{H}}_t^{-1} g_t(\tilde{\theta}_t)$
- 4: Compute $\tilde{\theta}_{t+1} = \arg \min_{\theta \in \Theta} \|\theta - \tilde{\theta}'_{t+1}\|_{\tilde{\mathcal{H}}_t}^2$
- 5: Update $\mathcal{H}_{t+1} = \mathcal{H}_t + H_t(\tilde{\theta}_{t+1})$

Output: $\tilde{\theta}_{t+1}$

Algorithm 2 Passive Data Collection

Input: Regularization λ , step size η

- 1: Initialize $\tilde{\theta}_1 = \mathbf{0}$ and $\tilde{\mathcal{H}}_1 = \lambda I$
- 2: **for** $t = 1, 2, \dots, T$ **do**
- 3: Observe preference data (x_t, a_t, a'_t, y_t)
- 4: $\tilde{\theta}_{t+1} = \text{Algorithm 1}(x_t, a_t, a'_t, y_t)$
- 5: **end for**
- 6: Construct $\tilde{J}_{T+1}(\pi)$ as in Eq. (6)

Output: $\pi_{T+1} = \arg \max_{\pi \in \Pi} \tilde{J}_{T+1}(\pi)$

standard OMD formulation updates using $g_t(\theta_t)$, whereas the implicit OMD updates the algorithm approximately with the subsequent sub-gradient, $g_t(\theta_{t+1})$. This distinction results in a notable gap in the convergence rates of the two methods. To this end, we propose to approximate the current loss $\ell_t(\theta)$ using a second-order Taylor expansion, drawing inspiration from [Zhang and Sugiyama \[2023\]](#). Define the second-order approximation of $\ell_t(\theta)$ as $\tilde{\ell}_t(\theta) = \ell_t(\tilde{\theta}_t) + g_t(\tilde{\theta}_t)^\top (\theta - \tilde{\theta}_t) + \frac{1}{2} \|\theta - \tilde{\theta}_t\|_{H_t(\tilde{\theta}_t)}^2$.

Then, we replace the loss $\ell_t(\theta)$ in Eq. (4) with the approximation $\tilde{\ell}_t(\theta)$, leading to the update rule:

$$\tilde{\theta}_{t+1} = \arg \min_{\theta \in \Theta} \left\{ \langle g_t(\tilde{\theta}_t), \theta \rangle + \frac{1}{2\eta} \|\theta - \tilde{\theta}_t\|_{\tilde{\mathcal{H}}_t}^2 \right\}, \quad (5)$$

where η is the step size and $\tilde{\mathcal{H}}_t = \mathcal{H}_t + \eta H_t(\tilde{\theta}_t)$ is the local norm with $\mathcal{H}_t \triangleq \sum_{i=1}^{t-1} H_i(\tilde{\theta}_{i+1}) + \lambda I$. Eq. (5) can be solved with a projected gradient step with the following equivalent form:

$$\tilde{\theta}'_{t+1} = \tilde{\theta}_t - \eta \tilde{\mathcal{H}}_t^{-1} g_t(\tilde{\theta}_t), \quad \tilde{\theta}_{t+1} = \arg \min_{\theta \in \Theta} \|\theta - \tilde{\theta}'_{t+1}\|_{\tilde{\mathcal{H}}_t}^2.$$

Thus, the estimator $\tilde{\theta}_{t+1}$ provides a closed-form solution, leading to a $\mathcal{O}(1)$ computational complexity per iteration. Since the estimator processes the samples in a one-pass manner, it mitigates the memory burden associated with computing the gradient of the full dataset. These properties make the method particularly suitable for edge devices, where both memory and computational resources are severely constrained. The detailed process of our proposed method is presented in Algorithm 1.

4.3 Theoretical Guarantee

Note that the update rule in Eq. (5) is a special case of online mirror descent, specifically:

$$\tilde{\theta}_{t+1} = \arg \min_{\theta \in \Theta} \left\{ \langle g_t(\tilde{\theta}_t), \theta \rangle + \frac{1}{\eta} \mathcal{D}_{\psi_t}(\theta, \tilde{\theta}_t) \right\},$$

where $\psi_t(\theta) = \frac{1}{2} \|\theta\|_{\tilde{\mathcal{H}}_t}^2$ is the regularizer and $\mathcal{D}_{\psi_t}(\theta, \tilde{\theta}_t) = \psi_t(\theta) - \psi_t(\tilde{\theta}_t) - \langle \nabla \psi_t(\tilde{\theta}_t), \theta - \tilde{\theta}_t \rangle$ is Bregman divergence. Based on the analysis of online mirror descent, we have the following lemma.

Lemma 1. *Let $\delta \in (0, 1]$, set $\eta = (1/2) \log 2 + (BL + 1)$ and $\lambda = 84\sqrt{2}\eta(dL^2 + BL^3)$, define $\mathcal{C}_t = \{\theta \in \Theta \mid \|\theta - \tilde{\theta}_t\|_{\mathcal{H}_t} \leq \tilde{\beta}_t \triangleq \mathcal{O}(\sqrt{d}(\log(t/\delta))^2)\}$. Then, we have $\Pr[\forall t \geq 1, \theta^* \in \mathcal{C}_t] \geq 1 - \delta$.*

Comparison with MLE. For the MLE estimator in Eq. (3), prior works [[Zhu et al., 2023](#), [Das et al., 2024](#), [Ji et al., 2024](#)] have shown $\|\theta - \tilde{\theta}_t\|_{V_t} \leq \tilde{\mathcal{O}}(\kappa\sqrt{d})$, where $V_t = \sum_{i=1}^{t-1} z_i z_i^\top + \lambda I$. By the definition of \mathcal{H}_t , it holds that $\mathcal{H}_t \succeq \kappa^{-1} V_t$, Lemma 1 implies $\|\theta - \tilde{\theta}_t\|_{V_t} \leq \sqrt{\kappa} \|\theta - \tilde{\theta}_t\|_{\mathcal{H}_t} \leq \tilde{\mathcal{O}}(\sqrt{\kappa d})$. This result shows that Lemma 1 improves upon previous bounds by at least a factor of $\sqrt{\kappa}$.

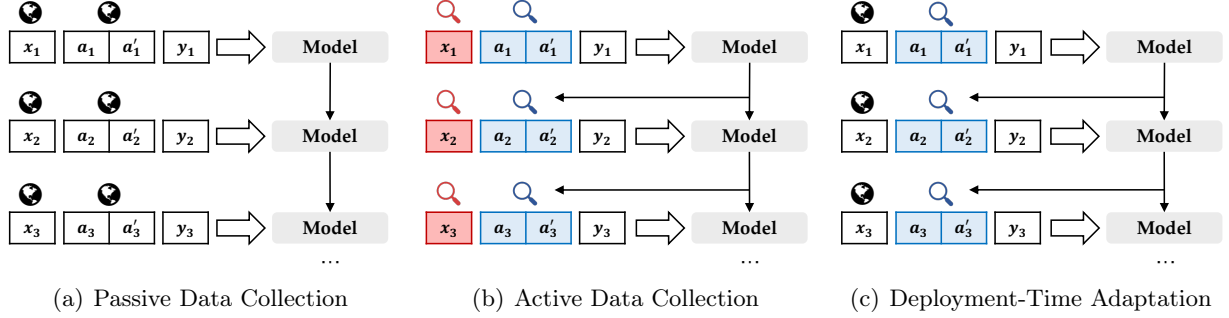


Figure 1: Different settings of online RLHF. Contexts and actions selected by the environment (🌐) are shown in grey, while those selected by the algorithm (🔍) are highlighted in color.

5 Applications in Three Online RLHF Scenarios

In this section, we apply our framework to three distinct RLHF scenarios, including online RLHF with passive data collection, active data collection, and deployment-time adaptation.

5.1 Online RLHF with Passive Data Collection

We first consider the passive data collection setting, where the algorithm can not control the data collection process. At each iteration, the learner obtains (x_t, a_t, a'_t, y_t) and updates by Eq. (5). We adopt the “pessimism in the face of uncertainty” principle and define the value function $\tilde{J}_{t+1}(\pi)$ as

$$\tilde{J}_{T+1}(\pi) = (\mathbb{E}_{x \sim \rho} [\phi(x, \pi(x))])^\top \tilde{\theta}_{T+1} - \tilde{\beta}_{T+1} \|\mathbb{E}_{x \sim \rho} [\phi(x, \pi(x))]\|_{\mathcal{H}_{T+1}^{-1}}. \quad (6)$$

where ρ is the context distribution. The policy π_{T+1} is selected as $\pi_{T+1} = \arg \max_{\pi \in \Pi} \tilde{J}_{T+1}(\pi)$. The detailed procedure is present in Algorithm 2, and we show it enjoys the following guarantee:

Theorem 1. *Set parameters as in Lemma 1, with probability at least $1 - \delta$, Algorithm 2 ensures*

$$\text{SubOpt}(\pi_{T+1}) = \mathbb{E}_{x \sim \rho} [r(x, \pi^*(x)) - r(x, \pi_{T+1}(x))] \leq \tilde{\mathcal{O}} \left(\sqrt{d} \cdot \|\mathbb{E}_{x \sim \rho} [\phi(x, \pi^*(x))]\|_{\mathcal{H}_{T+1}^{-1}} \right),$$

where ρ is the context distribution and π^* is the optimal policy.

Remark 2. The term $\|\mathbb{E}_{x \sim \rho} [\phi(x, \pi^*(x))]\|_{\mathcal{H}_{T+1}^{-1}}$ is referred to “concentrability coefficient” in the literature. It measures the distribution shift between the optimal policy and the collected data.

Remark 3. Our result improves upon Zhu et al. [2023] in both statistical and computational efficiency. Specifically, since $\mathcal{H}_t \succeq \kappa^{-1} V_t$, Theorem 2 directly implies a $\tilde{\mathcal{O}}(\sqrt{d\kappa} \cdot \|\mathbb{E}_{x \sim \rho} [\phi(x, \pi^*(x))]\|_{V_{T+1}^{-1}})$ guarantee, improving their $\tilde{\mathcal{O}}(\sqrt{d\kappa} \cdot \|\mathbb{E}_{x \sim \rho} [\phi(x, \pi^*(x))]\|_{V_{T+1}^{-1}})$ result by a factor of $\sqrt{\kappa}$. Regarding computational efficiency, their algorithm has a total storage complexity of $\mathcal{O}(T)$ and a time complexity of $\mathcal{O}(T \log T)$, leading to an amortized per-iteration cost of $\mathcal{O}(\log T)$. In contrast, our algorithm maintains a strict $\mathcal{O}(1)$ complexity per iteration, offering a substantial computational advantage.

Algorithm 3 Active Data Collection

Input: Regularization λ , step size η
1: Initialize $\tilde{\theta}_1 = \mathbf{0}$ and $\mathcal{H}_1 = \lambda I$
2: **for** $t = 1, 2, \dots, T$ **do**
3: Choose (x_t, a_t, a'_t) as Eq. (7), observe y_t
4: $\tilde{\theta}_{t+1} = \text{Algorithm 1}(x_t, a_t, a'_t, y_t)$
5: **end for**
6: Set $\tilde{r}_{T+1}(x, a) = \frac{1}{T+1} \sum_{t=1}^{T+1} \phi(x, a)^\top \tilde{\theta}_t$
Output: $\pi_{T+1}(x) = \arg \max_{a \in \mathcal{A}} \tilde{r}_{T+1}(x, a)$

Algorithm 4 Deployment-Time Adaptation

Input: Regularization λ , step size η
1: Initialize $\tilde{\theta}_1 = \mathbf{0}$ and $\mathcal{H}_1 = \lambda I$.
2: **for** $t = 1, 2, \dots, T$ **do**
3: Observes the context x_t .
4: Selects a_t and a'_t as Eq. (9) and Eq. (10)
5: Observe the preference feedback y_t
6: $\tilde{\theta}_{t+1} = \text{Algorithm 1}(x_t, a_t, a'_t, y_t)$
7: **end for**

5.2 Online RLHF with Active Data Collection

As established in Theorem 1, the sub-optimality gap depends on the concentrability coefficient, which quantifies the distributional mismatch between the optimal policy and the collected data. In this subsection, we propose an active data collection method that removes this dependency.

Active Data Collection. At each iteration, we obtain a new preference data (x_t, a_t, a'_t, y_t) . We then update the reward model using our one-pass reward modeling method as in Eq. (5). To guide data acquisition, we actively select the query with the highest uncertainty under the current reward model. Specifically, we select the next query by solving:

$$(x_{t+1}, a_{t+1}, a'_{t+1}) = \arg \max_{x, a, a' \in \mathcal{X} \times \mathcal{A} \times \mathcal{A}} \left\{ \left\| \phi(x, a) - \phi(x, a') \right\|_{\mathcal{H}_{t+1}^{-1}} \right\}. \quad (7)$$

Policy Optimization. After T rounds, we define the reward as the average of all the past estimations $\tilde{r}_{T+1}(x, a) = \frac{1}{T+1} \sum_{t=1}^{T+1} \phi(x, a)^\top \tilde{\theta}_t$. The policy is given by $\pi_{T+1}(x) = \arg \max_{a \in \mathcal{A}} \tilde{r}_{T+1}(x, a)$.

The detailed procedure is present in Algorithm 3. We show it enjoys the following guarantee.

Theorem 2. *Set parameters as in Lemma 1, with probability at least $1 - \delta$, Algorithm 3 ensures*

$$\text{SubOpt}(\pi_{T+1}) = \mathbb{E}_{x \sim \rho} [r(x, \pi^*(x)) - r(x, \pi_{T+1}(x))] \leq \tilde{\mathcal{O}}(d\sqrt{\kappa/T}),$$

where ρ is the context distribution and π^* is the optimal policy.

Remark 4. We attain the same sub-optimality gap as Das et al. [2024], but improve the computational efficiency significantly. Our algorithm has an $\mathcal{O}(1)$ time and space complexity per round, while their MLE estimator needs $\mathcal{O}(t \log t)$ time and $\mathcal{O}(t)$ space complexity at iteration t .

5.3 Online RLHF with Deployment-Time Adaptation

In this section, we consider the deployment-time adaptation setting, where users provide input contexts in an online manner, and the learner generates responses while simultaneously collecting feedback to improve the model. In this scenario, the learner faces a dual objective: selecting actions that maximize rewards to ensure a positive user experience, while also choosing actions that yield informative feedback to facilitate continual model improvement. To this end, we choose the cumulative regret as the performance measure, defined as

$$\text{Reg}_T = \sum_{t=1}^T \left(r(x_t, \pi^*(x_t)) - \frac{1}{2} (r(x_t, a_t) + r(x_t, a'_t)) \right), \quad (8)$$

where π^* is the optimal policy. This measure differs from the one introduced by Ji et al. [2024], which evaluates the gap between the optimal action and a single selected action. Our measure is designed to ensure that both actions are sufficiently effective, thereby delivering a high-quality user experience. While better aligns with deployment needs, it also poses greater challenges. Specifically, to optimize the measure in Ji et al. [2024], the learner can exploit one high-reward action while using the other for uniform exploration. In contrast, our setting imposes a stricter requirement: both actions must be good, thereby limiting the ability to sacrifice one action purely for exploration.

Action selection. At each iteration, given a new preference data (x_t, a_t, a'_t, y_t) , the learner updates the reward model using our one-pass reward modeling method as in Eq. (5). The learner must select queries that are both informative and with high rewards. To address this, we choose the first action a_{t+1} to maximize the estimated reward based on the estimator $\tilde{\theta}_{t+1}$, i.e.,

$$a_{t+1} = \arg \max_{a \in \mathcal{A}} \phi(x_{t+1}, a)^\top \tilde{\theta}_{t+1}. \quad (9)$$

The second action a'_{t+1} aims to maximize the reward and the distance between the two actions, i.e.,

$$a'_{t+1} = \arg \max_{a' \in \mathcal{A}} \{ \phi(x_{t+1}, a')^\top \tilde{\theta}_{t+1} + \tilde{\beta}_{t+1} \|\phi(x_{t+1}, a') - \phi(x_{t+1}, a_{t+1})\|_{\mathcal{H}_{t+1}^{-1}} \}. \quad (10)$$

The overall algorithm is summarized in Algorithm 4. We show it enjoys the following regret bound.

Theorem 3. *For any $\delta \in (0, 1]$, set parameters as in Lemma 1, Algorithm 4 ensures with probability at least $1 - \delta$, the regret satisfies*

$$\text{Reg}_T \leq \tilde{\mathcal{O}}(d\sqrt{\kappa T}).$$

Remark 5. Our result improves upon Saha et al. [2023] in both computational and statistical efficiency. Statistically, Theorem 3 improves their $\tilde{\mathcal{O}}(d\kappa\sqrt{T})$ result by a factor of $\sqrt{\kappa}$. Computationally, our algorithm has an $\mathcal{O}(1)$ time and space complexity per round, while their MLE estimator needs $\mathcal{O}(t \log t)$ time and $\mathcal{O}(t)$ space complexity at iteration t due to optimization over the historical data.

6 Practical Implementation

In this section, we introduce the practical implementation of our proposed algorithm.

6.1 Computation of Inverse Hessian

The OMD update in Eq. (5) requires computation of the inverse of the Hessian matrix. Omitting the projection operation, Eq. (5) can be rewritten as $\tilde{\theta}_{t+1} = \tilde{\theta}_t - \eta \tilde{\mathcal{H}}_t^{-1} g_t(\tilde{\theta}_t)$. Computing the full Hessian inverse $\tilde{\mathcal{H}}_t^{-1}$ directly incurs a time complexity of $\mathcal{O}(d^3)$, which is prohibitive for LLMs.

This cost can be reduced to $\mathcal{O}(d^2)$ by applying the Sherman-Morrison-Woodbury formula, leveraging the fact that the Hessian is a rank-one update. Specifically, for a matrix of the form $A + \mathbf{x}\mathbf{x}^\top$ where A is invertible and \mathbf{x} is a vector, the inverse is given by $(A + \mathbf{x}\mathbf{x}^\top)^{-1} = A^{-1} - \frac{A^{-1}\mathbf{x}\mathbf{x}^\top A^{-1}}{1 + \mathbf{x}^\top A^{-1}\mathbf{x}}$, requiring only $\mathcal{O}(d^2)$ time. Nevertheless, even this reduced complexity is costly for large models.

To further reduce the computational burden to $\mathcal{O}(d)$, we employ the Hessian-vector product technique combined with conjugate gradient descent [Boyd and Vandenberghe, 2004]. Instead of explicitly computing $\tilde{\mathcal{H}}_t^{-1}$, we solve the linear system $\tilde{\mathcal{H}}_t v = g_t(\tilde{\theta}_t)$ iteratively, where v is the solution

we seek. The HVP operation $\tilde{\mathcal{H}}_t v$ for any vector v can be computed efficiently using twice differentiation: $\tilde{\mathcal{H}}_t v = \nabla_{\theta}(\nabla_{\theta} \mathcal{L}_t(\theta)^{\top} v)|_{\theta=\tilde{\theta}_t} + \lambda_t v$, where $\mathcal{L}_t(\theta)$ is the function whose Hessian matrix at $\tilde{\theta}_t$ is $\tilde{\mathcal{H}}_t$. By leveraging this efficient computation, the conjugate gradient method iteratively refines the solution. In practice, finding $\mathcal{L}_t(\theta)$ is challenging as $\tilde{\mathcal{H}}_t = \mathcal{H}_t + \eta H_t(\tilde{\theta}_t)$ involve complex structure. A key insight is $\tilde{\mathcal{H}}_t$ can be viewed as the cumulative Hessian of the $\ell_t(\theta)$ approximately. This motivates the use of a more tractable surrogate $\ell_t(\theta)$ in Eq. (3) while keeping the update. To further approximate the effect of curvature accumulation, we adopt an adaptive damping scheme that approximately preserves historical Hessian information while incorporating new Hessian updates: $\lambda_t = \lambda_0 \cdot \min\{1, f(t/T)\}$, where $f(\cdot)$ is a monotonic increasing function, such as linear functions.

6.2 Computation of Model Uncertainty

In both online RLHF with active data collection and deployment-time adaptation, our algorithm utilizes uncertainty-driven query selection strategies. While quantifying uncertainty using the local norm induced by the Hessian matrix offers strong theoretical guarantees, it is computationally prohibitive in practice. To address this challenge, we adopt a rejection sampling-based approximation, a technique commonly employed for exploration in the literature [Nakano et al., 2021, Gulcehre et al., 2023, Dong et al., 2023, 2024]. Specifically, given a prompt, we sample n independent responses by the current model, then use the trained reward model to rank the responses. Then, we use different strategies to select the response for different settings. Specifically, In active data collection, the key insight is to identify and query samples that exhibit the greatest diversity in prompt action features. To this end, we select the response with the highest predicted reward and the response with the lowest predicted reward. In deployment-time adaptation, the core idea is to select the first action to maximize the estimated reward, while the second is chosen to balance high reward with sufficient divergence from the first. Concretely, we select the response with the highest predicted reward and another from the top-1/ q percentile of the reward, where q is a hyperparameter.

7 Experiments

In this section, we empirically evaluate the performance of our proposed method.¹ We first describe the experimental setup, and then present the empirical results.

7.1 Experiment setup

In our experiments, we employ the Llama-3-8B-Instruct² and Qwen2.5-7B-Instruct³ as the foundation model for reward model. We extract features $\phi(x, a)$ using the last layer of the model, and the dimension is $d = 4096$. We use two datasets for evaluation. The first one is Ultrafeedback-binarized dataset⁴, a pre-processed version of the original Ultrafeedback dataset [Cui et al., 2023], a widely used benchmark for RLHF. It collects about 64,000 prompts from diverse resources, including question answering, summarization, and dialogue generation. Each data consists of a context x , two responses a and a' , and a preference label y . We also employ a mixed dataset, Mixture2 dataset⁴, which combines a variety of preference datasets, including HH-RLHF, SHP, UltraFeedback, etc.

¹The code is available at https://github.com/ZinYY/Online_RLHF

²huggingface.co/meta-llama/Meta-Llama-3-8B-Instruct

³huggingface.co/Qwen/Qwen2.5-7B-Instruct

⁴huggingface.co/datasets/OpenRLHF/preference_dataset_mixture2_and_safe_pku

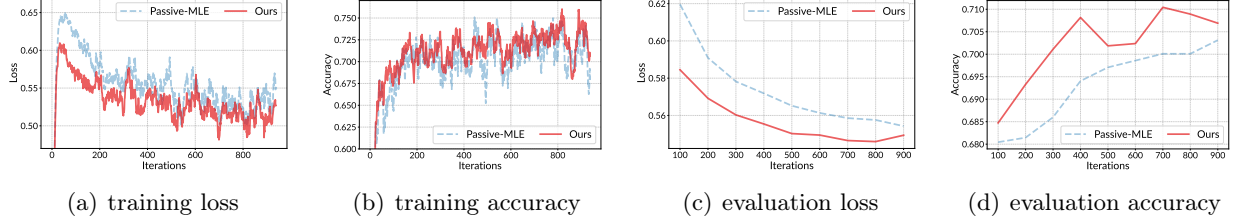


Figure 2: For **Llama-3-8B-Instruct** on Ultrafeedback-binarized dataset with passive data collection, we report the comparison of MLE and our OMD-based method for the reward model about (a) training loss, (b) training accuracy, (c) evaluation loss and (d) evaluation accuracy.

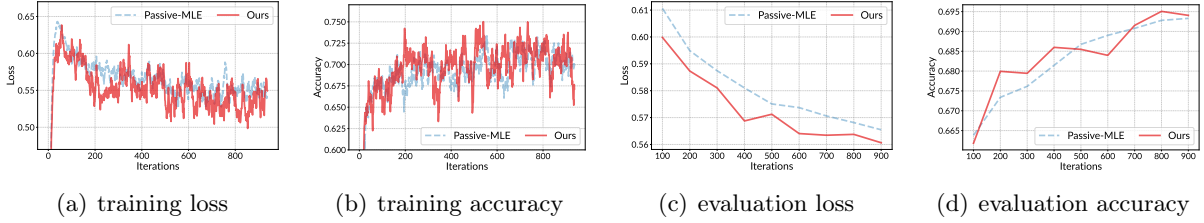


Figure 3: For **Qwen2.5-7B-Instruct** on Ultrafeedback-binarized dataset with passive data collection, we report the comparison of MLE and our OMD-based method for the reward model about (a) training loss, (b) training accuracy, (c) evaluation loss and (d) evaluation accuracy.

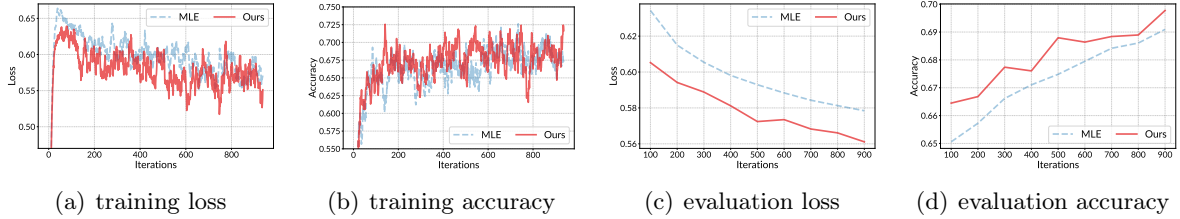


Figure 4: For **Llama-3-8B-Instruct** on Mixture2 dataset with passive data collection, we report the comparison of MLE and our OMD-based method for the reward model about (a) training loss, (b) training accuracy, (c) evaluation loss and (d) evaluation accuracy.

7.2 Experimental results

In this section, we present the experimental results, including passive data collection, active data collection and deployment-time adaptation.

7.2.1 Passive Data Collection

We randomly sample $T = 30,000$ data points from the dataset for training the reward model. We evaluate both the standard MLE-based method, which uses a stochastic gradient descent (SGD) optimizer, and our proposed OMD-based method in terms of reward model loss and accuracy. Figures 2, 3, and 4 present the results for three settings: (i) the **Llama-3-8B-Instruct** model on

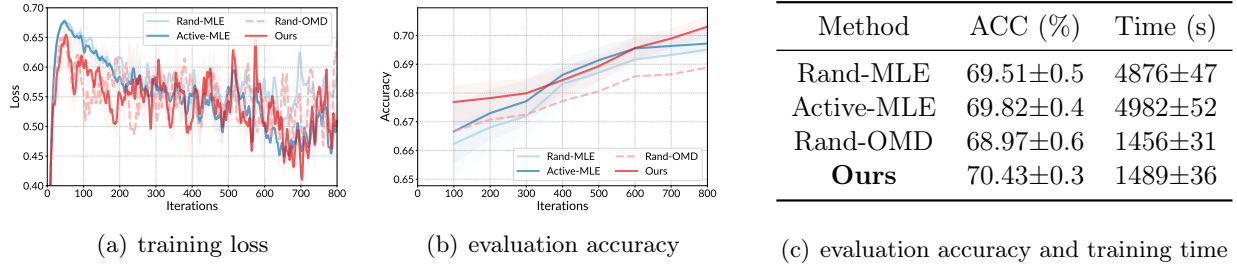


Figure 5: For **Llama-3-8B-Instruct** on Ultrafeedback-binarized dataset with active data collection, we report the comparison of different methods about (a) training loss, (b) evaluation accuracy and (c) final evaluation accuracy and training time.

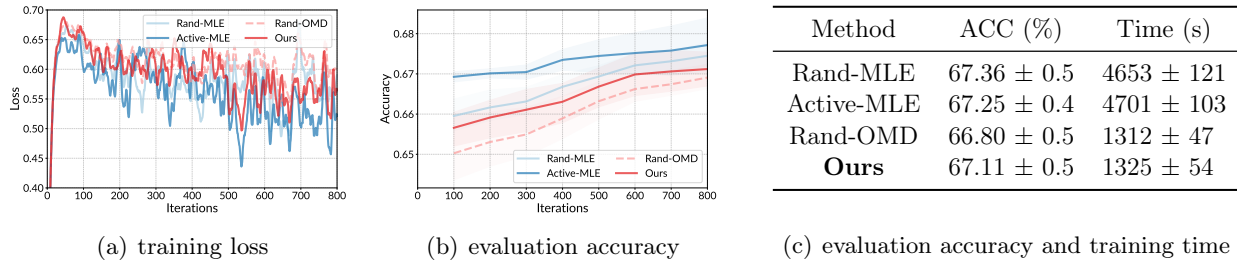


Figure 6: For **Qwen2.5-7B-Instruct** on Ultrafeedback-binarized dataset with active data collection, we report the comparison of different methods about (a) training loss, (b) evaluation accuracy and (c) final evaluation accuracy and training time.

the Ultrafeedback-binarized dataset, (ii) the **Qwen2.5-7B** model on the same dataset, and (iii) the **Llama-3-8B-Instruct** model on the Mixture2 dataset. We report the results across four key metrics: (a) training loss, (b) training accuracy, (c) evaluation loss and (d) evaluation accuracy. Our method demonstrates faster convergence to a lower loss and achieves higher evaluation accuracy compared to the MLE baseline. These results highlight the superior statistical efficiency of the OMD-based approach, which achieves improved performance with fewer training samples.

7.2.2 Active Data Collection

In this experimental setup, we constrain the algorithm to select only 6,400 samples from the full training dataset, based on different data selection strategies. We evaluate the performance of both the standard MLE-based method and our proposed OMD-based method under this limited data regime. To assess the effectiveness of the data selection strategy itself, we compare our approach against a random selection baseline. We report the results across four key metrics: (a) training loss curve, (b) evaluation accuracy curve and (c) final evaluation accuracy and training time. Figure 5 and Figure 6 demonstrate that our OMD-based method achieves competitive performance with the MLE-based method for both data collection strategies, while improving the training time by significantly. Moreover, our data selection strategy outperforms the random selection strategy, demonstrating that our method can effectively select informative data to improve the performance.

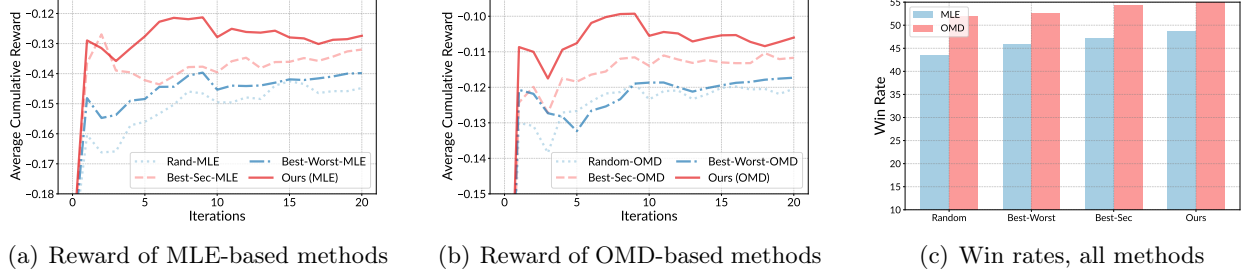


Figure 7: For **Llama-3-8B-Instruct** on Ultrafeedback-binarized dataset with deployment-time adaptation, we report (a) cumulative reward of MLE-based methods, (b) cumulative reward of OMD-based methods, and (c) win rates between MLE-based and OMD-based estimators with the same action selection strategy.

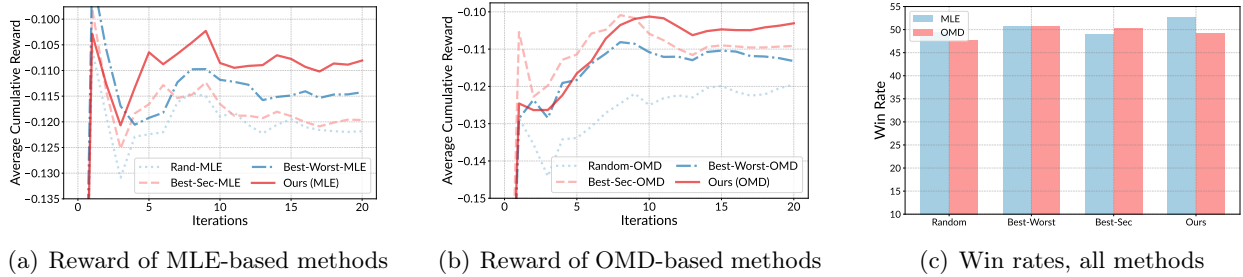


Figure 8: For **Qwen2.5-7B-Instruct** on Ultrafeedback-binarized dataset with deployment-time adaptation, we report (a) cumulative reward of MLE-based methods, (b) cumulative reward of OMD-based methods, and (c) win rates between MLE-based and OMD-based estimators with the same action selection strategy.

7.2.3 Deployment-Time Adaptation

To emulate real-world deployment scenarios, we partition the dataset into 20 sequential chunks and process them incrementally. This setup allows us to evaluate the adaptability and robustness of different action selection strategies over time. We benchmark our proposed selection strategy against three baselines: (i): random selection, (ii): the best and second best actions, and (iii): the best and worst actions. We combine the above strategies with MLE-based and OMD-based reward estimators. We report three key metrics: (a) the average cumulative reward for MLE-based methods, (b) the average cumulative reward for OMD-based methods, and (c) the win rate of OMD-based methods over MLE-based counterparts under identical selection strategies. As illustrated in Figure 7 and Figure 8, our action selection strategy consistently outperforms the baselines across both estimator types. These results highlight the strength of our approach in balancing the exploitation of high-reward responses with sufficient exploration to drive continual model improvement. Moreover, the win rate comparisons suggest that our OMD-based estimator shows competitive performance relative to its MLE-based counterpart, further validating its practical effectiveness.

8 Conclusion

In this work, we study the problem of online RLHF from the perspective of contextual bandits. To address the linear growth in computational complexity with respect to the number of iterations in reward modeling, we propose a novel one-pass reward modeling algorithm that achieves constant-time complexity per iteration. Our method is built upon the online mirror descent framework and incorporates a carefully designed local norm that captures second-order information. We apply our method to a broad range of online RLHF settings, including passive data collection, active data collection, and deployment-time adaptation, and design tailored algorithms for each scenario. We provide theoretical guarantees that our approach achieves superior statistical and computational efficiency relative to existing methods. Finally, we provide practical implementations of our method and conduct experiments using the **Llama-3-8B-Instruct** and **Qwen2.5-7B-Instruct** models on the Ultrafeedback-binarized and Mixture2 datasets, empirically validating its practical effectiveness.

While our work advances both the statistical and computational understanding of online RLHF, several important directions remain for future exploration. First, we assume a fixed feature mapping for the reward model; however, in practice, this mapping may evolve throughout the training process. Analyzing the impact of such dynamically changing feature representations presents a compelling direction for future research. Second, although our analysis is based on the Bradley-Terry model, extending the framework to other preference models, such as the Plackett-Luce model [Luce, 1959, Plackett, 1975], is another promising avenue that may broaden the applicability of our results.

References

- Yasin Abbasi-Yadkori, Dávid Pál, and Csaba Szepesvári. Improved algorithms for linear stochastic bandits. In *Advances in Neural Information Processing Systems 24 (NIPS)*, pages 2312–2320, 2011.
- Josh Achiam, Steven Adler, Sandhini Agarwal, Lama Ahmad, Ilge Akkaya, Florencia Leoni Aleman, Diogo Almeida, Janko Altschmidt, Sam Altman, Shyamal Anadkat, et al. GPT-4 technical report. *ArXiv preprint*, 2303.08774, 2023.
- Mohammad Gheshlaghi Azar, Zhaohan Daniel Guo, Bilal Piot, Rémi Munos, Mark Rowland, Michal Valko, and Daniele Calandriello. A general theoretical paradigm to understand learning from human preferences. In *Proceedings of the 27th International Conference on Artificial Intelligence and Statistics (AISTATS)*, pages 4447–4455, 2024.
- Yuntao Bai, Andy Jones, Kamal Ndousse, Amanda Askell, Anna Chen, Nova DasSarma, Dawn Drain, Stanislav Fort, Deep Ganguli, Tom Henighan, Nicholas Joseph, Saurav Kadavath, Jackson Kernion, Tom Conerly, Sheer El Showk, Nelson Elhage, Zac Hatfield-Dodds, Danny Hernandez, Tristan Hume, Scott Johnston, Shauna Kravec, Liane Lovitt, Neel Nanda, Catherine Olsson, Dario Amodei, Tom B. Brown, Jack Clark, Sam McCandlish, Chris Olah, Benjamin Mann, and Jared Kaplan. Training a helpful and harmless assistant with reinforcement learning from human feedback. *ArXiv preprint*, 2204.05862, 2022.
- Viktor Bengs, Aadirupa Saha, and Eyke Hüllermeier. Stochastic contextual dueling bandits under linear stochastic transitivity models. In *Proceedings of the 40th International Conference on Machine Learning (ICML)*, pages 1764–1786, 2022.

- Stephen P Boyd and Lieven Vandenberghe. *Convex optimization*. Cambridge University Press, 2004.
- Ralph Allan Bradley and Milton E Terry. Rank analysis of incomplete block designs: I. the method of paired comparisons. *Biometrika*, 39(3/4):324–345, 1952.
- Davide Cacciarelli and Murat Kulahci. Active learning for data streams: a survey. *Machine Learning*, 113(1):185–239, 2024.
- Nicolò Campolongo and Francesco Orabona. Temporal variability in implicit online learning. In *Advances in Neural Information Processing Systems 33 (NeurIPS)*, 2020.
- Shicong Cen, Jincheng Mei, Katayoon Goshvadi, Hanjun Dai, Tong Yang, Sherry Yang, Dale Schuurmans, Yuejie Chi, and Bo Dai. Value-incentivized preference optimization: A unified approach to online and offline RLHF. In *Proceedings of the 13th International Conference on Learning Representations (ICLR)*, 2025.
- Nicolò Cesa-Bianchi, Gábor Lugosi, and Gilles Stoltz. Minimizing regret with label efficient prediction. In *Proceedings of the 17th Conference on Learning Theory (COLT)*, pages 77–92, 2004.
- Nicolò Cesa-Bianchi, Claudio Gentile, and Luca Zaniboni. Worst-case analysis of selective sampling for linear classification. *Journal of Machine Learning Research*, 7:1205–1230, 2006.
- Paul F. Christiano, Jan Leike, Tom B. Brown, Miljan Martic, Shane Legg, and Dario Amodei. Deep reinforcement learning from human preferences. In *Advances in Neural Information Processing Systems 30 (NIPS)*, pages 4299–4307, 2017.
- Ganqu Cui, Lifan Yuan, Ning Ding, Guanming Yao, Wei Zhu, Yuan Ni, Guotong Xie, Zhiyuan Liu, and Maosong Sun. Ultrafeedback: Boosting language models with high-quality feedback. *ArXiv preprint*, 2310.01377, 2023.
- Nirjhar Das, Souradip Chakraborty, Aldo Pacchiano, and Sayak Ray Chowdhury. Active preference optimization for sample efficient RLHF. *ArXiv preprint*, 2402.10500, 2024.
- Hanze Dong, Wei Xiong, Deepanshu Goyal, Yihan Zhang, Winnie Chow, Rui Pan, Shizhe Diao, Jipeng Zhang, KaShun SHUM, and Tong Zhang. RAFT: Reward ranked finetuning for generative foundation model alignment. *Transactions on Machine Learning Research*, 2023. ISSN 2835-8856.
- Hanze Dong, Wei Xiong, Bo Pang, Haoxiang Wang, Han Zhao, Yingbo Zhou, Nan Jiang, Doyen Sahoo, Caiming Xiong, and Tong Zhang. RLHF workflow: From reward modeling to online RLHF. *Transactions on Machine Learning Research*, 2024.
- Miroslav Dudík, Katja Hofmann, Robert E. Schapire, Aleksandrs Slivkins, and Masrour Zoghi. Contextual dueling bandits. In *Proceedings of The 28th Conference on Learning Theory (COLT)*, pages 563–587, 2015.
- Louis Faury, Marc Abeille, Kwang-Sung Jun, and Clément Calauzènes. Jointly efficient and optimal algorithms for logistic bandits. In *Proceedings of the 25th International Conference on Artificial Intelligence and Statistics (AISTATS)*, pages 546–580, 2022.

- Yoav Freund, H Sebastian Seung, Eli Shamir, and Naftali Tishby. Selective sampling using the query by committee algorithm. *Machine learning*, 28:133–168, 1997.
- Caglar Gulcehre, Tom Le Paine, Srivatsan Srinivasan, Ksenia Konyushkova, Lotte Weerts, Abhishek Sharma, Aditya Siddhant, Alex Ahern, Miaosen Wang, Chenjie Gu, Wolfgang Macherey, Arnaud Doucet, Orhan Firat, and Nando de Freitas. Reinforced self-training (rest) for language modeling. *ArXiv preprint*, 2308.08998, 2023.
- Shangmin Guo, Biao Zhang, Tianlin Liu, Tianqi Liu, Misha Khalman, Felipe Llinares, Alexandre Ramé, Thomas Mesnard, Yao Zhao, Bilal Piot, Johan Ferret, and Mathieu Blondel. Direct language model alignment from online AI feedback. *ArXiv preprint*, 2402.04792, 2024.
- Sheng-Jun Huang, Rong Jin, and Zhi-Hua Zhou. Active learning by querying informative and representative examples. In *Advances in Neural Information Processing Systems 23 (NIPS)*, pages 892–900, 2010.
- Kaixuan Ji, Jiafan He, and Quanquan Gu. Reinforcement learning from human feedback with active queries. *ArXiv preprint*, 2402.09401, 2024.
- Diederik P Kingma and Jimmy Ba. Adam: A method for stochastic optimization. In *Proceedings of 3rd International Conference on Learning Representations (ICLR)*, 2015.
- Joongkyu Lee and Min-hwan Oh. Nearly minimax optimal regret for multinomial logistic bandit. In *Advances in Neural Information Processing Systems 36 (NeurIPS)*, page to appear, 2024.
- Long-Fei Li, Yu-Jie Zhang, Peng Zhao, and Zhi-Hua Zhou. Provably efficient reinforcement learning with multinomial logit function approximation. In *Advances in Neural Information Processing Systems 37 (NeurIPS)*, page to appear, 2024.
- Llama Team. The llama 3 herd of models. *ArXiv preprint*, 2407.21783, 2023.
- R Duncan Luce. *Individual Choice Behavior: A Theoretical Analysis*. Wiley, 1959.
- Reiichiro Nakano, Jacob Hilton, Suchir Balaji, Jeff Wu, Long Ouyang, Christina Kim, Christopher Hesse, Shantanu Jain, Vineet Kosaraju, William Saunders, et al. Webgpt: Browser-assisted question-answering with human feedback. *ArXiv preprint*, 2112.09332, 2021.
- Long Ouyang, Jeffrey Wu, Xu Jiang, Diogo Almeida, Carroll Wainwright, Pamela Mishkin, Chong Zhang, Sandhini Agarwal, Katarina Slama, Alex Ray, et al. Training language models to follow instructions with human feedback. *Advances in Neural Information Processing Systems 35 (NeurIPS)*, pages 27730–27744, 2022.
- Junsoo Park, Seungyeon Jwa, Meiying Ren, Daeyoung Kim, and Sanghyuk Choi. Offsetbias: Leveraging debiased data for tuning evaluators. *ArXiv preprint*, 2407.06551, 2024.
- Robin L Plackett. The analysis of permutations. *Journal of the Royal Statistical Society Series C: Applied Statistics*, 24(2):193–202, 1975.
- Qwen Team. Qwen2.5 technical report. *ArXiv preprint*, 2412.15115, 2024.

- Rafael Rafailov, Archit Sharma, Eric Mitchell, Christopher D. Manning, Stefano Ermon, and Chelsea Finn. Direct preference optimization: Your language model is secretly a reward model. In *Advances in Neural Information Processing Systems 36 (NeurIPS)*, pages 53728–53741, 2023.
- Aadirupa Saha. Optimal algorithms for stochastic contextual preference bandits. In *Advances in Neural Information Processing Systems 34 (NeurIPS)*, pages 30050–30062, 2021.
- Aadirupa Saha, Aldo Pacchiano, and Jonathan Lee. Dueling RL: reinforcement learning with trajectory preferences. In *Proceedings of the 26th International Conference on Artificial Intelligence and Statistics (AISTATS)*, pages 6263–6289, 2023.
- John Schulman, Filip Wolski, Prafulla Dhariwal, Alec Radford, and Oleg Klimov. Proximal policy optimization algorithms. *ArXiv preprint*, 1707.06347, 2017.
- Ayush Sekhari, Karthik Sridharan, Wen Sun, and Runzhe Wu. Contextual bandits and imitation learning with preference-based active queries. In *Advances in Neural Information Processing Systems 36 (NeurIPS)*, page to appear, 2024.
- Burr Settles. Active learning literature survey. *Technical Report*, 2009.
- H Sebastian Seung, Manfred Opper, and Haim Sompolinsky. Query by committee. In *Proceedings of the 5th Annual Conference on Computational Learning Theory*, pages 287–294, 1992.
- Hugo Touvron, Louis Martin, Kevin Stone, Peter Albert, Amjad Almahairi, Yasmine Babaei, Nikolay Bashlykov, Soumya Batra, Prajjwal Bhargava, Shruti Bhosale, et al. Llama 2: Open foundation and fine-tuned chat models. *ArXiv preprint*, 2307.09288, 2023.
- Quoc Tran-Dinh, Yen-Huan Li, and Volkan Cevher. Composite convex minimization involving self-concordant-like cost functions. In *Proceedings of the 3rd International Conference on Modelling, Computation and Optimization in Information Systems and Management Sciences*, pages 155–168, 2015.
- Arun Verma, Zhongxiang Dai, Xiaoqiang Lin, Patrick Jaillet, and Bryan Kian Hsiang Low. Neural dueling bandits: Preference-based optimization with human feedback. In *Proceedings of the 13th International Conference on Learning Representations (ICLR)*, 2025.
- Yue Wu, Zhiqing Sun, Huizhuo Yuan, Kaixuan Ji, Yiming Yang, and Quanquan Gu. Self-play preference optimization for language model alignment. In *Proceedings of the 13th International Conference on Learning Representations (ICLR)*, 2025.
- Tengyang Xie, Dylan J Foster, Akshay Krishnamurthy, Corby Rosset, Ahmed Awadallah, and Alexander Rakhlin. Exploratory preference optimization: Harnessing implicit q^* -approximation for sample-efficient rlhf. In *Proceedings of the 13th International Conference on Learning Representations (ICLR)*, 2025.
- Wei Xiong, Hanze Dong, Chenlu Ye, Ziqi Wang, Han Zhong, Heng Ji, Nan Jiang, and Tong Zhang. Iterative preference learning from human feedback: Bridging theory and practice for RLHF under KL-constraint. In *Proceedings of the 41st International Conference on Machine Learning (ICML)*, pages 54715–54754, 2024.

- Weizhe Yuan, Richard Yuanzhe Pang, Kyunghyun Cho, Xian Li, Sainbayar Sukhbaatar, Jing Xu, and Jason Weston. Self-rewarding language models. In *Proceedings of the 41st International Conference on Machine Learning (ICML)*, 2024.
- Yisong Yue, Josef Broder, Robert Kleinberg, and Thorsten Joachims. The K-armed dueling bandits problem. *Journal of Computer and System Sciences*, 78(5):1538–1556, 2012.
- Shenao Zhang, Donghan Yu, Hiteshi Sharma, Han Zhong, Zhihan Liu, Ziyi Yang, Shuohang Wang, Hany Hassan Awadalla, and Zhaoran Wang. Self-exploring language models: Active preference elicitation for online alignment. *Transactions on Machine Learning Research*, 2025. ISSN 2835-8856.
- Yu-Jie Zhang and Masashi Sugiyama. Online (multinomial) logistic bandit: Improved regret and constant computation cost. In *Advances in Neural Information Processing Systems 36 (NeurIPS)*, pages 29741–29782, 2023.
- Banghua Zhu, Michael Jordan, and Jiantao Jiao. Principled reinforcement learning with human feedback from pairwise or K-wise comparisons. In *Proceedings of the 40th International Conference on Machine Learning (ICML)*, pages 43037–43067, 2023.

A Useful Lemmas

Lemma 2. For any $t \in [T]$, define the second-order approximation of the loss function $\ell_t(\theta)$ at the estimator $\tilde{\theta}_t$ as $\tilde{\ell}_t(\theta) = \ell_t(\tilde{\theta}_t) + \langle \nabla \ell_t(\tilde{\theta}_t), \theta - \tilde{\theta}_t \rangle + \frac{1}{2} \|\theta - \tilde{\theta}_t\|_{\mathcal{H}_t}^2$. Then, for the following update rule

$$\tilde{\theta}_{t+1} = \arg \min_{\theta \in \Theta} \left\{ \tilde{\ell}_t(\theta) + \frac{1}{2\eta} \|\theta - \tilde{\theta}_t\|_{\mathcal{H}_t}^2 \right\},$$

it holds that

$$\begin{aligned} & \|\tilde{\theta}_{t+1} - \theta^*\|_{\mathcal{H}_{t+1}}^2 \\ & \leq 2\eta \left(\sum_{i=1}^t \ell_i(\theta^*) - \sum_{i=1}^t \ell_i(\tilde{\theta}_{i+1}) \right) + 4\lambda B^2 + 12\sqrt{2}BL^3\eta \sum_{i=1}^t \|\tilde{\theta}_{i+1} - \tilde{\theta}_i\|_2^2 - \sum_{i=1}^t \|\tilde{\theta}_{i+1} - \tilde{\theta}_i\|_{\mathcal{H}_i}^2. \end{aligned}$$

Proof. Based on the analysis of (implicit) OMD update (see Lemma 5), for any $i \in [T]$, we have

$$\langle \nabla \tilde{\ell}_i(\tilde{\theta}_{i+1}), \tilde{\theta}_{i+1} - \theta^* \rangle \leq \frac{1}{2\eta} \left(\|\tilde{\theta}_i - \theta^*\|_{\mathcal{H}_i}^2 - \|\tilde{\theta}_{i+1} - \theta^*\|_{\mathcal{H}_i}^2 - \|\tilde{\theta}_{i+1} - \tilde{\theta}_i\|_{\mathcal{H}_i}^2 \right)$$

According to Lemma 6, we have

$$\ell_i(\tilde{\theta}_{i+1}) - \ell_i(\theta^*) \leq \langle \nabla \ell_i(\tilde{\theta}_{i+1}), \tilde{\theta}_{i+1} - \theta^* \rangle - \frac{1}{\zeta} \|\tilde{\theta}_{i+1} - \theta^*\|_{\nabla^2 \ell_i(\tilde{\theta}_{i+1})}^2,$$

where $\zeta = \log 2 + 2(LB + 1)$. Then, by combining the above two inequalities, we have

$$\begin{aligned} \ell_i(\tilde{\theta}_{i+1}) - \ell_i(\theta^*) & \leq \langle \nabla \ell_i(\tilde{\theta}_{i+1}) - \nabla \tilde{\ell}_i(\tilde{\theta}_{i+1}), \tilde{\theta}_{i+1} - \theta^* \rangle \\ & \quad + \frac{1}{\zeta} \left(\|\tilde{\theta}_i - \theta^*\|_{\mathcal{H}_i}^2 - \|\tilde{\theta}_{i+1} - \theta^*\|_{\mathcal{H}_{i+1}}^2 - \|\tilde{\theta}_{i+1} - \tilde{\theta}_i\|_{\mathcal{H}_i}^2 \right). \end{aligned}$$

We can further bound the first term of the right-hand side as:

$$\begin{aligned} \langle \nabla \ell_i(\tilde{\theta}_{i+1}) - \nabla \tilde{\ell}_i(\tilde{\theta}_{i+1}), \tilde{\theta}_{i+1} - \theta^* \rangle & = \langle \nabla \ell_i(\tilde{\theta}_{i+1}) - \nabla \ell_i(\tilde{\theta}_i) - \nabla^2 \ell_i(\tilde{\theta}_i)(\tilde{\theta}_{i+1} - \tilde{\theta}_i), \tilde{\theta}_{i+1} - \theta^* \rangle \\ & = \langle D^3 \ell_i(\xi_{i+1})\tilde{\theta}_{i+1} - \tilde{\theta}_i, \tilde{\theta}_{i+1} - \theta^* \rangle \\ & \leq 3\sqrt{2}L \|\tilde{\theta}_{i+1} - \theta^*\|_2 \|\tilde{\theta}_{i+1} - \tilde{\theta}_i\|_{\nabla^2 \ell_i(\xi_{i+1})}^2 \\ & \leq 6\sqrt{2}BL \|\tilde{\theta}_{i+1} - \tilde{\theta}_i\|_{\nabla^2 \ell_i(\xi_{i+1})}^2 \\ & \leq 6\sqrt{2}BL^3 \|\tilde{\theta}_{i+1} - \tilde{\theta}_i\|_2^2, \end{aligned}$$

where the second equality holds by the mean value theorem, the first inequality holds by the self-concordant-like property of $\ell_i(\cdot)$ in Lemma 3, and the last inequality holds by $\tilde{\theta}_{i+1}$ and θ^* belong to $\Theta = \{\theta \in \mathbb{R}^d, \|\theta\|_2 \leq B\}$, and $\nabla^2 \ell_i(\xi_{i+1}) \preceq L^2 I_d$.

Then, by taking the summation over i and rearranging the terms, we obtain

$$\begin{aligned} & \|\tilde{\theta}_{t+1} - \theta^*\|_{\mathcal{H}_{t+1}}^2 \\ & \leq \zeta \sum_{i=1}^t \left(\ell_i(\theta^*) - \ell_i(\tilde{\theta}_{i+1}) \right) + \|\tilde{\theta}_1 - \theta^*\|_{\mathcal{H}_1}^2 + 6\sqrt{2}BL^3\zeta \sum_{i=1}^t \|\tilde{\theta}_{i+1} - \tilde{\theta}_i\|_2^2 - \sum_{i=1}^t \|\tilde{\theta}_{i+1} - \tilde{\theta}_i\|_{\mathcal{H}_i}^2 \\ & \leq \zeta \sum_{i=1}^t \left(\ell_i(\theta^*) - \ell_i(\tilde{\theta}_{i+1}) \right) + 4\lambda B^2 + 6\sqrt{2}BL^3\zeta \sum_{i=1}^t \|\tilde{\theta}_{i+1} - \tilde{\theta}_i\|_2^2 - \sum_{i=1}^t \|\tilde{\theta}_{i+1} - \tilde{\theta}_i\|_{\mathcal{H}_i}^2, \end{aligned}$$

where the last inequality is by $\|\tilde{\theta}_1 - \theta^*\|_{\mathcal{H}_1}^2 \leq \lambda \|\tilde{\theta}_1 - \theta^*\|_2^2 \leq 4\lambda B^2$. Set $\zeta = 2\eta$ ends the proof. \blacksquare

B Proof of Lemma 1

Proof. Based on Lemma 2, we have

$$\begin{aligned} & \|\tilde{\theta}_{t+1} - \theta^*\|_{\mathcal{H}_{t+1}}^2 \\ & \leq 2\eta \left(\sum_{i=1}^t \ell_i(\theta^*) - \sum_{i=1}^t \ell_i(\tilde{\theta}_{i+1}) \right) + 4\lambda B^2 + 12\sqrt{2}BL^3\eta \sum_{i=1}^t \|\tilde{\theta}_{i+1} - \tilde{\theta}_i\|_2^2 - \sum_{i=1}^t \|\tilde{\theta}_{i+1} - \tilde{\theta}_i\|_{\mathcal{H}_i}^2. \end{aligned}$$

It remains to bound the right-hand side of the above inequality in the following. The most challenging part is to bound the term $\sum_{i=1}^t \ell_i(\theta^*) - \sum_{i=1}^t \ell_i(\tilde{\theta}_{i+1})$. This term might seem straightforward to control, as it can be observed that $\theta^* = \arg \min_{\theta \in \mathbb{R}^d} \bar{\ell}(\theta) \triangleq \mathbb{E}_{y_i}[\ell_i(\theta)]$, where $\ell_i(\theta)$ serves as an empirical observation of $\bar{\ell}(\theta)$. Consequently, the loss gap term seemingly can be bounded using appropriate concentration results. However, a caveat lies in the fact that the update of the estimator $\tilde{\theta}_{i+1}$ depends on ℓ_i , or more precisely y_i , making it difficult to directly apply such concentrations.

To address this issue, following the analysis in Zhang and Sugiyama [2023], we decompose the loss gap into two components by introducing an intermediate term. Specifically, we define the softmax function as $[\sigma_i(q)]_1 = \frac{\exp(q)}{1+\exp(q)}$ and $[\sigma_i(q)]_0 = \frac{1}{1+\exp(q)}$, where $[\cdot]_i$ denotes the i -th element of the vector. Then, the loss function $\ell_i(\theta)$ can be rewritten as

$$\ell(q_t, y_t) = -\mathbb{1}_{\{y_t=1\}} \cdot \log([\sigma(q_t)]_1) - \mathbb{1}_{\{y_t=0\}} \cdot \log([\sigma(q_t)]_0).$$

Then, we define the pseudo-inverse function of $\sigma^{-1}(p)$ with $[\sigma^{-1}(p)]_1 = \log(q/(1-q))$ and $[\sigma^{-1}(p)]_0 = \log((1-p)/p)$. Then, we decompose the regret into two terms by introducing an intermediate term.

$$\sum_{i=1}^t \ell_i(\theta^*) - \sum_{i=1}^t \ell_i(\tilde{\theta}_{i+1}) = \underbrace{\sum_{i=1}^t \ell_i(\theta^*) - \sum_{i=1}^t \ell_i(q_i, y_i)}_{\text{term (a)}} + \underbrace{\sum_{i=1}^t \ell_i(q_i, y_i) - \sum_{i=1}^t \ell_i(\tilde{\theta}_{i+1})}_{\text{term (b)}}$$

where q_i is an aggregating forecaster for logistic loss defined by $q_i = \sigma^{-1}(\mathbb{E}_{\theta \sim P_i}[\sigma(\theta^\top z_i)])$ and $P_i = \mathcal{N}(\tilde{\theta}_i, (1 + c\mathcal{H}_i^{-1}))$ is the Gaussian distribution with mean $\tilde{\theta}_i$ and covariance $(1 + c\mathcal{H}_i^{-1})$, where $c > 0$ is a constant to be specified later. It remains to bound the terms **term (a)** and **term (b)**, which were initially analyzed in Zhang and Sugiyama [2023] and further refined by Lee and Oh [2024]. Specifically, using Lemmas F.2 and F.3 in Lee and Oh [2024], we can bound them as follows.

For **term (a)**, let $\delta \in (0, 1)$ and $\lambda \geq 1$. With probability at least $1 - \delta$, for all $t \in [T]$, we have

$$\text{term (a)} \leq (3\log(1+2t) + 2 + LB) \left(\frac{17}{16}\lambda + 2\sqrt{\lambda} \log \left(\frac{2\sqrt{1+2t}}{\delta} \right) + 16 \left(\log \left(\frac{2\sqrt{1+2t}}{\delta} \right) \right)^2 \right) + 2.$$

For **term (b)**, let $\lambda \geq \max\{2, 72cd\}$. Then, for all $t \in [T]$, we have

$$\text{term (b)} \leq \frac{1}{2c} \sum_{i=1}^t \|\tilde{\theta}_{i+1} - \tilde{\theta}_i\|_{\mathcal{H}_i}^2 + \sqrt{6cd} \log \left(1 + \frac{2tB^2}{d\lambda} \right)$$

Combing the above two bounds, we have

$$\|\tilde{\theta}_{t+1} - \theta^*\|_{\mathcal{H}_{t+1}}^2 \leq 12\sqrt{2}BL^3\eta \sum_{i=1}^t \|\tilde{\theta}_{i+1} - \tilde{\theta}_i\|_2^2 + \left(\frac{\eta}{c} - 1 \right) \sum_{i=1}^t \|\tilde{\theta}_{i+1} - \tilde{\theta}_i\|_{\mathcal{H}_i}^2 + C.$$

where $C = 2\eta(3\log(1+2t) + 2 + BL) \left(\frac{17}{16}\lambda + 2\sqrt{\lambda} \log \left(\frac{2\sqrt{1+2t}}{\delta} \right) + 16 \left(\log \left(\frac{2\sqrt{1+2t}}{\delta} \right) \right)^2 \right) + 4\eta + 2\eta\sqrt{6}cd \log \left(1 + \frac{2tL^2}{d\lambda} \right) + 4\lambda B^2$. Setting $c = 7\eta/6$ and $\lambda \geq 84\sqrt{2}BL^3\eta$, we have

$$\begin{aligned} & 12\sqrt{2}BL^3\eta \sum_{i=1}^t \left\| \tilde{\theta}_{i+1} - \tilde{\theta}_i \right\|_2^2 + \left(\frac{\eta}{c} - 1 \right) \sum_{i=1}^t \left\| \tilde{\theta}_{i+1} - \tilde{\theta}_i \right\|_{\mathcal{H}_i}^2 \\ & \leq \left(12\sqrt{2}BL^3\eta - \frac{\lambda}{7} \right) \sum_{i=1}^t \left\| \tilde{\theta}_{i+1} - \tilde{\theta}_i \right\|_2^2 \\ & \leq 0. \end{aligned}$$

Note that $84\sqrt{2}(BL^3 + dL^2)\eta \geq \max\{2L^2, 72cdL^2, 84\sqrt{2}BL^3\eta\}$, so we set $\lambda \geq 84\sqrt{2}(BL^3 + dL^2)\eta$. As we have $\eta = (1/2)\log 2 + (BL + 1)$, we have

$$\left\| \tilde{\theta}_{t+1} - \theta^* \right\|_{\mathcal{H}_{t+1}} \leq \mathcal{O}\left(\sqrt{d}(\log(t/\delta))^2\right).$$

This finishes the proof. ■

C Proof of Theorem 1

Proof. Define $J(\pi) = \mathbb{E}_{x \sim \rho}[r(x, \pi(x))]$, we have

$$\text{SubOpt}(\pi_T) = \left(J(\pi^*) - \tilde{J}(\pi^*) \right) + \left(\tilde{J}(\pi^*) - \tilde{J}(\pi_T) \right) + \left(\tilde{J}(\pi_T) - J(\pi_T) \right).$$

Since π_T is the optimal policy under expected value $\tilde{J}(\pi)$, i.e., $\tilde{J}(\pi_T) = \max_{\pi \in \Pi} \tilde{J}(\pi)$, we have

$$\tilde{J}(\pi^*) - \tilde{J}(\pi_T) \leq 0 \tag{11}$$

For the third term, we have with probability at least $1 - \delta$, it holds that

$$\tilde{J}(\pi_T) - J(\pi_T) = \min_{\theta \in \mathcal{C}_T} \mathbb{E}_{x \sim \rho} \left[\theta^\top \phi(s, \pi_T(s)) \right] - \mathbb{E}_{x \sim \rho} \left[\theta^{*\top} \phi(s, \pi_T(s)) \right] \leq 0, \tag{12}$$

where the last inequality holds by $\theta^* \in \mathcal{C}_T$ with probability at least $1 - \delta$.

For the first term, we have with probability at least $1 - \delta$, it holds that

$$\begin{aligned} J(\pi^*) - \tilde{J}(\pi^*) &= \mathbb{E}_{x \sim \rho} \left[(\theta^*)^\top \phi(s, \pi^*(s)) \right] - \min_{\theta \in \mathcal{C}_T} \mathbb{E}_{x \sim \rho} \left[\theta^\top \phi(s, \pi^*(s)) \right] \\ &= \sup_{\theta \in \mathcal{C}_T} \mathbb{E}_{x \sim \rho} \left[\left(\theta^* - \tilde{\theta}_T + \tilde{\theta}_T - \theta \right)^\top \phi(x, \pi^*(x)) \right] \\ &= \mathbb{E}_{x \sim \rho} \left[\left(\theta^* - \tilde{\theta}_T \right)^\top \phi(x, \pi^*(x)) \right] + \sup_{\theta \in \mathcal{C}_T} \mathbb{E}_{x \sim \rho} \left[\left(\tilde{\theta}_T - \theta \right)^\top \phi(x, \pi^*(x)) \right] \\ &\leq \left(\left\| \theta^* - \tilde{\theta}_T \right\|_{\mathcal{H}_T} + \sup_{\theta \in \mathcal{C}_T} \left\| \theta - \tilde{\theta}_T \right\|_{\mathcal{H}_T} \right) \cdot \left\| \mathbb{E}_{x \sim \rho} [\phi(x, \pi^*(x))] \right\|_{\mathcal{H}_T^{-1}}, \end{aligned}$$

where the first inequality holds by the Cauchy-Schwarz inequality.

Since it holds $\theta^* \in \mathcal{C}_T$ with probability at least $1 - \delta$ by Lemma 1, we have $\|\theta^* - \tilde{\theta}_T\|_{\mathcal{H}_T} \leq \tilde{\beta}_T$ and $\sup_{\theta \in \mathcal{C}_T} \|\theta - \tilde{\theta}_T\|_{\mathcal{H}_T} \leq \tilde{\beta}_T$. Thus, we obtain

$$J(\pi^*) - \tilde{J}(\pi^*) \leq 2\tilde{\beta}_T \cdot \|\mathbb{E}_{x \sim \rho}[\phi(x, \pi^*(x))]\|_{\mathcal{H}_T^{-1}}. \quad (13)$$

Combining Eq. (11), Eq. (12), and Eq. (13) and substituting $\tilde{\beta}_T = \mathcal{O}(\sqrt{d}(\log(T/\delta))^2)$, we have with probability at least $1 - \delta$, it holds that

$$\text{SubOpt}(\pi_T) \leq 2\tilde{\beta}_T \cdot \|\mathbb{E}_{x \sim \rho}[\phi(x, \pi^*(x))]\|_{\mathcal{H}_T^{-1}} \leq \mathcal{O}\left(\sqrt{d}\left(\log \frac{T}{\delta}\right)^2 \cdot \|\mathbb{E}_{x \sim \rho}[\phi(x, \pi^*(x))]\|_{\mathcal{H}_T^{-1}}\right).$$

This completes the proof. \blacksquare

D Proof of Theorem 2

Proof. Let the sub-optimality gap for a context $x \in \mathcal{X}$ be denoted as $\text{SubOpt}(x)$. Thus, for any $\delta \in (0, 1)$, with probability at least $1 - \delta$, we have

$$\begin{aligned} \text{SubOpt}(x) &= (\phi(x, \pi^*(x)) - \phi(x, \pi_T(x)))^\top \theta^* \\ &\leq (\phi(x, \pi^*(x)) - \phi(x, \pi_T(x)))^\top \theta^* + (\phi(x, \pi_T(x)) - \phi(x, \pi^*(x)))^\top \left(\frac{1}{T} \sum_{t=1}^T \tilde{\theta}_t\right) \\ &= (\phi(x, \pi^*(x)) - \phi(x, \pi_T(x)))^\top \left(\theta^* - \frac{1}{T} \sum_{t=1}^T \tilde{\theta}_t\right) \\ &= \frac{1}{T} \sum_{t=1}^T (\phi(x, \pi^*(x)) - \phi(x, \pi_T(x)))^\top (\theta^* - \tilde{\theta}_t) \\ &\leq \frac{1}{T} \sum_{t=1}^T \|\phi(x, \pi^*(x)) - \phi(x, \pi_T(x))\|_{\mathcal{H}_t^{-1}} \|\theta^* - \tilde{\theta}_t\|_{\mathcal{H}_t} \\ &\leq \frac{\tilde{\beta}_T}{T} \sum_{t=1}^T \|\phi(x, \pi^*(x)) - \phi(x, \pi_T(x))\|_{\mathcal{H}_t^{-1}}, \end{aligned}$$

where the first inequality is due to the fact that $(\phi(x, \pi_T(x)) - \phi(x, \pi^*(x)))^\top \left(\frac{1}{T} \sum_{t=1}^T \tilde{\theta}_t\right) \geq 0$ by the design of $\pi_T(x)$, the second is due to the Cauchy-Schwarz inequality, and the last inequality is due to $\|\theta^* - \tilde{\theta}_t\|_{\mathcal{H}_t} \leq \beta_T$ with probability at least $1 - \delta$ by Lemma 1.

By our algorithm's choice $(x_t, a_t, a'_t) = \arg \max_{x \in \mathcal{X}, a, a' \in \mathcal{A}} \|\phi(x, a) - \phi(x, a')\|_{\mathcal{H}_t^{-1}}$, we have

$$\sum_{t=1}^T \|\phi(x, \pi^*(x)) - \phi(x, \pi_T(x))\|_{\mathcal{H}_t^{-1}} \leq \sum_{t=1}^T \|\phi(x_t, a_t) - \phi(x_t, a'_t)\|_{\mathcal{H}_t^{-1}} = \sum_{t=1}^T \|z_t\|_{\mathcal{H}_t^{-1}}.$$

Furthermore, by the definition of \mathcal{H}_t , we have

$$\mathcal{H}_t = \lambda I_d + \sum_{s=1}^{t-1} \dot{\sigma} \left(z_s^\top \tilde{\theta}_{s+1} \right) z_s z_s^\top \geq \lambda I_d + \frac{1}{\kappa} \sum_{s=1}^{t-1} z_s z_s^\top = \frac{1}{\kappa} \left(\kappa \lambda I_d + \sum_{s=1}^{t-1} z_s z_s^\top \right) = \frac{1}{\kappa} V_t.$$

Thus, we have

$$\sum_{t=1}^T \|z_t\|_{\mathcal{H}_t^{-1}} \leq \sqrt{\kappa} \sum_{t=1}^T \|z_t\|_{V_t^{-1}} \leq \sqrt{\kappa} \sqrt{T \sum_{t=1}^T \|z_t\|_{V_t^{-1}}^2} \leq \sqrt{2\kappa d T \log \left(1 + \frac{4TL^2}{\lambda\kappa d}\right)},$$

where the first inequality holds by the fact that $\mathcal{H}_t \succeq \frac{1}{\kappa} V_t$, the second inequality holds by the Cauchy-Schwarz inequality, and the last inequality holds by the elliptic potential lemma in Lemma 4. Thus, we have for any context $x \in \mathcal{X}$,

$$\text{SubOpt}(x) \leq \frac{\tilde{\beta}_T}{T} \sqrt{2\kappa d T \log \left(1 + \frac{4TL^2}{\lambda\kappa d}\right)}.$$

By the definition of $\text{SubOpt}(\pi_T)$, we have with probability at least $1 - \delta$,

$$\text{SubOpt}(\pi_T) = \mathbb{E}_{x \sim \rho} [\text{SubOpt}(x)] \leq \frac{\tilde{\beta}_T}{T} \sqrt{2\kappa d T \log \left(1 + \frac{T}{\lambda\kappa d}\right)} \leq \tilde{\mathcal{O}} \left(d \sqrt{\frac{\kappa}{T}}\right).$$

This finishes the proof. ■

E Proof of Theorem 3

Proof. We first analyze the instantaneous regret at round t . For any $\delta \in (0, 1)$, with probability at least $1 - \delta$, it holds that

$$\begin{aligned} & (r(x_t, \pi^*(x_t)) - r(x_t, a_t)) + (r(x_t, \pi^*(x_t)) - r(x_t, a'_t)) \\ &= (\phi(x_t, \pi^*(x_t)) - \phi(x_t, a_t))^\top \theta^* + (\phi(x_t, \pi^*(x_t)) - \phi(x_t, a'_t))^\top \theta^* \\ &= 2(\phi(x_t, \pi^*(x_t)) - \phi(x_t, a_t))^\top \theta^* + (\phi(x_t, a_t) - \phi(x_t, a'_t))^\top \theta^* \\ &= 2(\phi(x_t, \pi^*(x_t)) - \phi(x_t, a_t))^\top (\theta^* - \tilde{\theta}_t) + 2(\phi(x_t, \pi^*(x_t)) - \phi(x_t, a_t))^\top \tilde{\theta}_t \\ &\quad + (\phi(x_t, a_t) - \phi(x_t, a'_t))^\top (\theta^* - \tilde{\theta}_t) + (\phi(x_t, a_t) - \phi(x_t, a'_t))^\top \tilde{\theta}_t \\ &\leq 2\|\phi(x_t, \pi^*(x_t)) - \phi(x_t, a_t)\|_{\mathcal{H}_t^{-1}} \|\theta^* - \tilde{\theta}_t\|_{\mathcal{H}_t} + (\phi(x_t, \pi^*(x_t)) - \phi(x_t, a_t))^\top \tilde{\theta}_t \\ &\quad + \|\phi(x_t, a_t) - \phi(x_t, a'_t)\|_{\mathcal{H}_t^{-1}} \|\theta^* - \tilde{\theta}_t\|_{\mathcal{H}_t} + (\phi(x_t, a_t) - \phi(x_t, a'_t))^\top \tilde{\theta}_t \\ &\leq 2\tilde{\beta}_t \|\phi(x_t, \pi^*(x_t)) - \phi(x_t, a_t)\|_{\mathcal{H}_t^{-1}} + (\phi(x_t, \pi^*(x_t)) - \phi(x_t, a'_t))^\top \tilde{\theta}_t \\ &\quad + \tilde{\beta}_t \|\phi(x_t, a_t) - \phi(x_t, a'_t)\|_{\mathcal{H}_t^{-1}} \\ &\leq 2\tilde{\beta}_t \|\phi(x_t, a'_t) - \phi(x_t, a_t)\|_{\mathcal{H}_t^{-1}} + (\phi(x_t, a'_t) - \phi(x_t, \pi^*(x_t)))^\top \tilde{\theta}_t \\ &\quad + (\phi(x_t, \pi^*(x_t)) - \phi(x_t, a'_t))^\top \tilde{\theta}_t + \tilde{\beta}_t \|\phi(x_t, a_t) - \phi(x_t, a'_t)\|_{\mathcal{H}_t^{-1}} \\ &= 3\tilde{\beta}_t \|\phi(x_t, a_t) - \phi(x_t, a'_t)\|_{\mathcal{H}_t^{-1}}, \end{aligned}$$

where the first inequality holds by the Holder's inequality and the arm selection strategy of a_t such that $(\phi(x_t, \pi^*(x_t)) - \phi(x_t, a_t))^\top \tilde{\theta}_t \leq (\phi(x_t, a_t) - \phi(x_t, a'_t))^\top \tilde{\theta}_t$, the second inequality holds by $\tilde{\theta}_t \in \mathcal{C}_t$ with probability

at least $1 - \delta$ by Lemma 1, the third inequality holds by arm selection strategy of a'_t such that $a'_t = \arg \max_{a \in \mathcal{A}} \phi(x_t, a)^\top \tilde{\theta}_t + 2\tilde{\beta} \|\phi(x_t, a) - \phi(x_t, a_t)\|_{\mathcal{H}_t^{-1}}$.

By the definition of \mathcal{H}_t , we have

$$\mathcal{H}_t = \lambda I_d + \sum_{s=1}^{t-1} \dot{\sigma} \left(z_s^\top \tilde{\theta}_{s+1} \right) z_s z_s^\top \geq \lambda I_d + \frac{1}{\kappa} \sum_{s=1}^{t-1} z_s z_s^\top = \frac{1}{\kappa} \left(\kappa \lambda I_d + \sum_{s=1}^{t-1} z_s z_s^\top \right) = \frac{1}{\kappa} V_t.$$

Thus, we have

$$\sum_{t=1}^T \|z_t\|_{\mathcal{H}_t^{-1}} \leq \sqrt{\kappa} \sum_{t=1}^T \|z_t\|_{V_t^{-1}} \leq \sqrt{\kappa} \sqrt{T \sum_{t=1}^T \|z_t\|_{V_t^{-1}}^2} \leq \sqrt{2\kappa d T \log \left(1 + \frac{4TL^2}{\lambda \kappa d} \right)},$$

where the first inequality holds by the fact that $\mathcal{H}_t \succeq \frac{1}{\kappa} V_t$, the second inequality holds by the Cauchy-Schwarz inequality, and the last inequality holds by the elliptic potential lemma in Lemma 4.

Therefore, we have

$$\text{Reg}_T \leq \frac{3}{2} \tilde{\beta}_T \sqrt{2\kappa d T \log \left(1 + \frac{4\kappa T L^2}{\lambda d} \right)} \leq \tilde{\mathcal{O}}(d\sqrt{\kappa T}).$$

where the This completes the proof. ■

F Supporting Lemmas

Definition 3 (Tran-Dinh et al. [2015]). A convex function $f \in C^3(\mathbb{R}^m)$ is M -self-concordant-like function if

$$|\psi'''(s)| \leq M \|\mathbf{b}\|_2 \psi''(s),$$

for $s \in \mathbb{R}$ and $M > 0$, where $\psi(s) := f(\mathbf{a} + s\mathbf{b})$ for any $\mathbf{a}, \mathbf{b} \in \mathbb{R}^m$.

Lemma 3 (Lee and Oh [2024, Proposition C.1]). The loss $\ell_t(\theta)$ defined in Eq. (3) is $3\sqrt{2}L$ -self-concordant-like for $\forall t \in [T]$.

Lemma 4 (Abbasi-Yadkori et al. [2011, Lemma 11]). Suppose $x_1, \dots, x_t \in \mathbb{R}^d$ and for any $1 \leq s \leq t$, $\|x_s\|_2 \leq L$. Let $V_t = \lambda I_d + \sum_{s=1}^{t-1} x_s x_s^\top$ for $\lambda \geq 0$. Then, we have $\sum_{s=1}^t \|x_s\|_{V_s^{-1}}^2 \leq 2d \log \left(1 + \frac{tL^2}{\lambda d} \right)$.

Lemma 5 (Campolongo and Orabona [2020, Proposition 4.1]). Define \mathbf{w}_{t+1} as the solution of

$$\mathbf{w}_{t+1} = \arg \min_{\mathbf{w} \in \mathcal{V}} \{ \eta \ell_t(\mathbf{w}) + \mathcal{D}_\psi(\mathbf{w}, \mathbf{w}_t) \},$$

where $\mathcal{V} \subseteq \mathcal{W} \subseteq \mathbb{R}^d$ is a non-empty convex set. Further supposing $\psi(\mathbf{w})$ is 1-strongly convex w.r.t. a certain norm $\|\cdot\|$ in \mathcal{W} , then there exists a $\mathbf{g}'_t \in \partial \ell_t(\mathbf{w}_{t+1})$ such that

$$\langle \eta_t \mathbf{g}'_t, \mathbf{w}_{t+1} - \mathbf{u} \rangle \leq \langle \nabla \psi(\mathbf{w}_t) - \nabla \psi(\mathbf{w}_{t+1}), \mathbf{w}_{t+1} - \mathbf{u} \rangle$$

for any $\mathbf{u} \in \mathcal{W}$.

Lemma 6 (Zhang and Sugiyama [2023, Lemma 1]). Let $\ell(\mathbf{z}, y) = \sum_{k=0}^K \mathbf{1}\{y = k\} \cdot \log \left(\frac{1}{[\sigma(\mathbf{z})]_k} \right)$ where $\sigma(\mathbf{z})_k = \frac{e^{z_k}}{\sum_{j=0}^K e^{z_j}}$, $\mathbf{a} \in [-C, C]^K$, $y \in \{0\} \cup [K]$ and $\mathbf{b} \in \mathbb{R}^K$ where $C > 0$. Then, we have

$$\ell(\mathbf{a}, y) \geq \ell(\mathbf{b}, y) + \nabla \ell(\mathbf{b}, y)^\top (\mathbf{a} - \mathbf{b}) + \frac{1}{\log(K+1) + 2(C+1)} (\mathbf{a} - \mathbf{b})^\top \nabla^2 \ell(\mathbf{b}, y) (\mathbf{a} - \mathbf{b}).$$

G Details of Experiments

In this section, we provide the omitted details of the experiment details and additional results.

G.1 Implementation Details

Datasets. We use the UltraFeedback-binarized dataset [Rafailov et al., 2023] for the experiments. This dataset is derived from the original UltraFeedback dataset, which comprises 64,000 prompts sourced from diverse datasets including UltraChat, ShareGPT, Evol-Instruct, TruthfulQA, FalseQA, and FLAN. For each prompt, four model completions were generated using various open-source and proprietary language models, with GPT-4 providing comprehensive evaluations across multiple criteria including helpfulness, honesty, and truthfulness. The binarized version was constructed by selecting the completion with the highest overall score as the "chosen" response and randomly selecting one of the remaining completions as the "rejected" response, creating clear preference pairs suitable for reward modeling and direct preference optimization. This dataset structure aligns well with our experimental setup, providing a robust foundation for evaluating different preference learning approaches. The dataset's diverse prompt sources and evaluation criteria make it particularly valuable for training and evaluating reward models in a real-world context. To further tailor the dataset to our experimental setup, we organize the dataset as follows:

- Online RLHF with *passive data collection*: We randomly sample $T = 30,000$ data points from the UltraFeedback-binarized dataset's `train_prefs` split for training. Each data point consists of a prompt and two responses with a binary preference label indicating the preferred response. We use the `test_prefs` split for evaluation.
- Online RLHF with *active data collection*: We allow the method to actively select 6,400 samples from the `train_prefs` split according to different selection strategies. The global batch size is set to 8 for training. The selection is performed iteratively, where in each iteration, the method selects the most informative samples based on its selection criterion.
- Deployment-time adaption: We use a pre-processed online variant of the UltraFeedback-binarized dataset from the `test_gen` split. The dataset is divided into 20 sequential chunks to simulate an online deployment scenario. For each chunk, we generate responses using the current policy (the foundation model of policy model is chosen to be `meta-llama / Llama-3.2-1B`), evaluate them using both the learned reward model and an oracle reward model. We choose `NCSOFT/Llama-3-OffsetBias-RM-8B` [Park et al., 2024] as the oracle reward model. After each chunk, we use the policy model to randomly generate 64 responses using different seeds. We then apply various strategies (*Random*, *Best-Two*, etc.) to select responses and construct new preference pairs, which are then used to update the reward model and the policy model.

Practical Implementation. To efficiently implement the OMD update in Eq. (5) without the costly computing and storing the full Hessian matrix, we utilize the Hessian-vector product (HVP) method combined with conjugate gradient descent. The key insight is that the update can be reformulated as solving a linear system. For the OMD update:

$$\tilde{\theta}_{t+1} = \arg \min_{\theta \in \Theta} \left\{ \langle g_t(\tilde{\theta}_t), \theta \rangle + \frac{1}{2\eta} \|\theta - \tilde{\theta}_t\|_{\tilde{\mathcal{H}}_t}^2 \right\} \approx \tilde{\theta}_t - \eta \tilde{\mathcal{H}}_t^{-1} g_t(\tilde{\theta}_t),$$

Algorithm 5 Efficient Update using Hessian-Vector Product with Conjugate Gradient

Input: Current parameter $\tilde{\theta}_t$, gradient $g_t(\tilde{\theta}_t)$, learning rate η , max CG steps K , base damping λ_0 , error tolerance ϵ

- 1: Initialize $v_0 = 0$, $r_0 = g_t(\tilde{\theta}_t)$, $p_0 = r_0$
- 2: Compute damping $\lambda_t = \lambda_0 \cdot \min\{1, f(t/T)\}$
- 3: **for** $k = 0, 1, \dots, K - 1$ **do**
- 4: Compute HVP: $\tilde{\mathcal{H}}_t p_k = \nabla_{\theta}(\nabla_{\theta} \mathcal{L}(\theta)^{\top} p_k)|_{\theta=\tilde{\theta}_t} + \lambda_t p_k$
- 5: $\alpha_k = \frac{r_k^{\top} r_k}{p_k^{\top} \tilde{\mathcal{H}}_t p_k}$, $v_{k+1} = v_k + \alpha_k p_k$, $r_{k+1} = r_k - \alpha_k \tilde{\mathcal{H}}_t p_k$,
- 6: $\beta_{k+1} = \frac{r_{k+1}^{\top} r_{k+1}}{r_k^{\top} r_k}$, $p_{k+1} = r_{k+1} + \beta_{k+1} p_k$
- 7: **if** $\|r_{k+1}\| \leq \epsilon$ **then**
- 8: **break**
- 9: **end if**
- 10: **end for**
- 11: Update parameter: $\tilde{\theta}_{t+1} = \tilde{\theta}_t - \eta v_K$

Output: Updated parameter $\tilde{\theta}_{t+1}$

where we ignore the projection operation. The key challenge is computing $\tilde{\mathcal{H}}_t^{-1} g_t(\tilde{\theta}_t)$ efficiently. Instead of explicitly computing $\tilde{\mathcal{H}}_t^{-1}$, we solve the linear system $\tilde{\mathcal{H}}_t v = g_t(\tilde{\theta}_t)$

$$\tilde{\mathcal{H}}_t v = g_t(\tilde{\theta}_t),$$

where v is the solution we seek. We use the conjugate gradient method with a damped Hessian to solve this system iteratively. The HVP operation $\tilde{\mathcal{H}}_t v$ for any vector v can be computed efficiently using automatic differentiation $\tilde{\mathcal{H}}_t v = \nabla_{\theta}(\nabla_{\theta} \mathcal{L}(\theta)^{\top} v)|_{\theta=\tilde{\theta}_t} + \lambda v$, where λ is a damping coefficient that ensures numerical stability and $\mathcal{L}(\theta)$ is the loss function. The full algorithm is summarized in Algorithm 5. To ensure stability and convergence, we employ an adaptive damping strategy as $\lambda_t = \lambda_0 \cdot \min\{1, f(t/T)\}$, where $f(\cdot)$ is a damping growth function that can be linear, logarithmic, or cosine. In practice, we set $K = 3$ and $\lambda_0 = 0.8$ for all experiments.

G.2 Validating the Magnitude of κ

We validate the magnitude of κ by computing its value during the training process. The results show that $\kappa = 171.62 \pm 85.49$ during our training process, which is relatively large.

G.3 Combined with Adam Optimizer

In previous experiments, we used SGD to update model parameters. In this section, we integrate the methods with the *Adam optimizer* [Kingma and Ba, 2015], i.e., adding the first and second momentum terms to the model updates. The results, shown in Figure 9, indicate that the Adam optimizer further enhances the performance of our method by leveraging the momentum term to accelerate convergence. With the momentum term, our method remains superior to the MLE-based method; however, the performance gap is reduced. We think that this is because the Adam optimizer incorporates second-order information for optimization, diminishing the advantage of our method compared to the SGD cases.

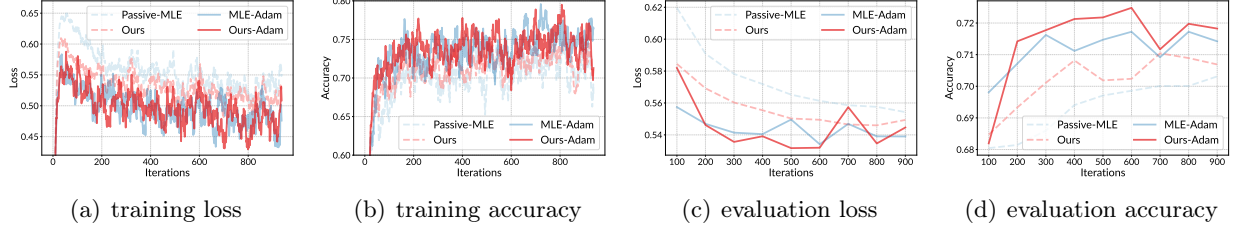


Figure 9: For online RLHF with *passive data collection*, we compare our proposed method and MLE [Zhu et al., 2023] in with passive data collection combined with *Adam*. We report the average accuracy and loss of the reward model during the training process.

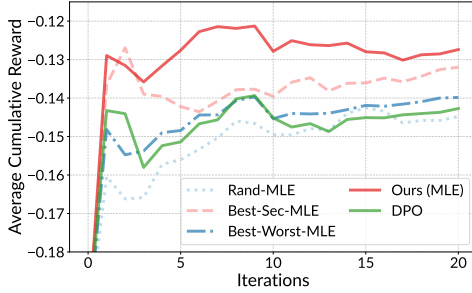


Figure 10: Comparison of DPO and our method in deployment-time adaptation.

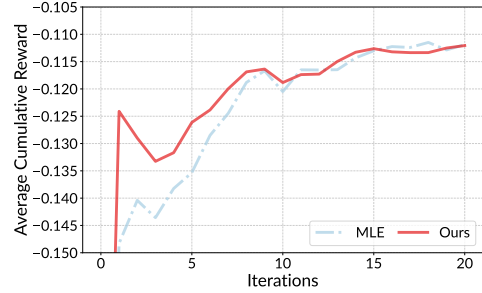


Figure 11: Comparison of different methods for full update in deployment-time adaptation.

G.4 Comparison with DPO

We also compare with DPO [Rafailov et al., 2023] in the deployment stage, as a reward-free method, DPO optimizes the policy directly using preference feedback without explicit reward modeling. To ensure a fair comparison, we initialize the policy with 400 samples and use the same dataset settings as PPO to iteratively update the policy model using the DPO algorithm. The results are illustrated in Figure 10. While DPO outperforms the random baseline (Rand-MLE), it achieves lower cumulative rewards than the methods using our action selection. This result suggests that DPO’s online learning capability remains a challenge. In contrast, the reward model learned by our selection strategy effectively learned streaming data and continuously updates the policy as new data arrive, indicating that in our deployment stage, a reward model with PPO may be a more suitable choice for sequentially learning from new data.

G.5 Full Update of Reward Model

Figure 11 shows deployment-time adaptation results using the *meta-llama/Llama-3.2-1B* model, where we update all parameters of the reward model instead of only the final layer. Both our method and MLE use the same action selection strategy. Our approach achieves comparable performance with MLE, indicating that our OMD-based method is still compatible with full-model updates.